Title: 800,000 years of abrupt climate variability*

Authors: Stephen Barker[1**], Gregor Knorr[2], R. Lawrence Edwards[3], Frédéric Parrenin[4,5], Aaron E. Putnam[6], Luke C. Skinner[7], Eric Wolff[8] and Martin Ziegler[1]

[1]School of Earth and Ocean Sciences, Cardiff University, Main Building, Park Place, Cardiff CF10 3AT, UK

[2]Alfred Wegener Institute, 27570 Bremerhaven, Germany

[3]Department of Earth Sciences, University of Minnesota, Minneapolis, MN 55455, USA

[4]Laboratoire de Glaciologie, CNRS and Joseph Fourier University, 38400 Grenoble, France

[5]Laboratoire Chrono-Environnement, 25000 Besançon, France

[6]Department of Earth Sciences and Climate Change Institute, University of Maine, Orono, ME 04469, US0041

[7]Godwin Laboratory for Palaeoclimate Research, Department of Earth Sciences, University of Cambridge, Downing Street, Cambridge CB2 3EQ, UK

[8]British Antarctic Survey, Madingley Road, High Cross, Cambridge CB3 0ET, UK

**corresponding author, email: barkers3@cf.ac.uk

*This manuscript was published in Science. This version has not undergone final editing. Please refer to the complete version of record at http://www.sciencemag.org/. The manuscript may not be reproduced or used in any manner that does not fall within the fair use provisions of the Copyright Act without the prior, written permission of AAAS

The final version of the manuscript is available here:

https://doi.org/10.1126/science.1203580

800,000 years of abrupt climate variability

Stephen Barker[1*], Gregor Knorr[2], R. Lawrence Edwards[3], Frédéric Parrenin[4,5], Aaron E. Putnam[6], Luke C. Skinner[7], Eric Wolff[8] and Martin Ziegler[1]

[1]School of Earth and Ocean Sciences, Cardiff University, Main Building, Park Place, Cardiff CF10 3AT, UK

[2]Alfred Wegener Institute, 27570 Bremerhaven, Germany

[3]Department of Earth Sciences, University of Minnesota, Minneapolis, MN 55455, USA

[4]Laboratoire de Glaciologie, CNRS and Joseph Fourier University, 38400 Grenoble, France

[5]Department of Earth Sciences and Climate Change Institute, University of Maine, Orono, ME 04469, US0041

[6]Laboratoire Chrono-Environnement, 25000 Besançon, France

[7]Godwin Laboratory for Palaeoclimate Research, Department of Earth Sciences, University of Cambridge, Downing Street, Cambridge CB2 3EQ, UK

[8]British Antarctic Survey, Madingley Road, High Cross, Cambridge CB3 0ET, UK

*corresponding author, email: barkers3@cf.ac.uk

Abstract

We construct an 800 kyr synthetic record of Greenland climate variability based on the thermal bipolar seesaw model. Our Greenland analogue reproduces much of the variability seen in the Greenland ice cores over the last 100 kyr. We also find a strong similarity with the absolutely-dated speleothem record from China, allowing us to place ice core records within an absolute timeframe for the last 400 kyr. The synthetic record provides both a stratigraphic reference and a conceptual basis for assessing the long-term evolution of millennial-scale variability, and its potential role in longer timescale climate change. Indeed, we provide evidence for a ubiquitous association between bipolar seesaw oscillations and glacial terminations throughout the Middle to Late Pleistocene.

Main text (2,214 words)

Ice core records from Greenland first demonstrated the existence of repeated, large and abrupt shifts in Northern Hemisphere climate during the last ice age (*1, 2*). These shifts are one expression of a global system, capable of driving major changes in components ranging from ocean temperatures (*3, 4*) to monsoon rainfall (*5*). The Greenland records provide an archetypal view of abrupt climate variability (*6*) over the last glacial cycle, which was characterised by rapid alternations between cold (stadial) and warmer (interstadial) conditions (known as Dansgaard-Oeschger, D-O, oscillations). But, ironically, the great temporal resolution of these records makes it difficult to look further back in time; the high accumulation rates on the Greenland ice sheet mean that over 3,000 meters of ice may represent just 100,000 years of climate history. Fortunately, climate records preserved in Antarctic ice (*7*) enable us here to address this fundamental problem.

The (thermal) bipolar seesaw model (*8, 9*) attempts to explain the observed relationship between millennial-scale temperature variability observed in Greenland and Antarctica by calling on variations in the strength of the Atlantic meridional overturning circulation (AMOC). The northward heat transport associated with this circulation (*10*) implies that changes in the strength of overturning should lead to opposing temperature responses in either hemisphere. According to the seesaw model, a transition from weak to strong AMOC would cause an abrupt warming across the North Atlantic region (a D-O warming event) while temperatures across Antarctica would (in general) shift from warming to cooling. The ocean / atmosphere climate system is an integrated and synergistic system and it is important to note that the overall concept of the bipolar seesaw we invoke here is not restricted to oceanic processes but also includes atmospheric shifts that may be related to the variations we are interested in (*9, 11-14*).

The thermal bipolar seesaw model implies an antiphase relationship between the Greenland temperature anomaly and the rate of change of Antarctic temperature (*9*). This can be illustrated by a lead/lag analysis of the methane-tuned temperature records after removal of their orbital-timescale variability (*6*) (Greenland, GL_T_hi, and Antarctica, AA_T_hi) and the first time derivative of Antarctic temperature, AA_T_hi' (Fig. 1). Comparison of the undifferentiated records illustrates the historical debate as to whether the two signals are positively correlated with a southern lead of 1000-1600 years or negatively correlated with the north leading by 400-800 years (*15, 16*). However, as implied by the study of (*9*) and illustrated in Fig. 1, a near zero-phase anti-correlation is observed between GL_T_hi and AA_T_hi'. Uncertainties in the ice age-gas age offset (Δage), which may be up to hundreds of years (*17*), mean that an exact antiphase relationship is unlikely to be observed (*6*). As described by (*18*), using a similar approach, the process of differentiating amplifies noise in the original temperature record. Smoothing the record of AA_T_hi before differentiating reduces this noise but will compromise the ability of AA_T_hi' to replicate the abrupt nature of D-O warming events and reduce the predicted amplitude of smaller events. The choice of smoothing window is therefore a trade-off between these effects (*6*) (Fig. 1).

The empirical relations illustrated in Fig. 1 present the possibility to produce a synthetic record of Greenland climate using the Antarctic record, with the purpose of reconstructing the nature of northern variability beyond the present limit of the Greenland records. The record of Greenland temperature (GL_T) is broken down into its orbital and millennial-timescale components, GL_T_lo and GL_T_hi respectively (Figs. 2, S5), where GL_T_lo is a 7 kyr smooth of GL_T (*6*) and GL_T_hi is the difference between GL_T and GL_T_lo. We consider GL_T_hi as the northern temperature anomaly with respect to mean background conditions. Building on Fig. 1 we assume that the rate of Antarctic temperature change is inversely proportional to the northern temperature anomaly. We therefore scale the amplitude of AA_T_hi' to match that of GL_T_hi over the last 90 kyr to produce a synthetic record of northern millennial-scale temperature variability, GL_T_syn_hi (Fig. 2C) (*6*). It can be seen that a synthetic reconstruction of GL_T could be made by combining GL_T_syn_hi with an estimate for GL_T_lo. The orbital-timescale components of the Greenland and Antarctic temperature records (GL_T_lo and AA_T_lo respectively) are highly correlated, with the southern record leading the north by ~2000 years (*6*). We therefore incorporate longer timescale variations into our reconstruction by substituting GL_T_lo with a scaled version of AA_T_lo, shifted by 2000 yr (which we call GL_T_syn_lo) (Fig. S5) (*6*). Our full reconstruction, GL_T_syn, (Fig. 2D) is then the sum of GL_T_syn_lo and GL_T_syn_hi.

Our formulation of the thermal bipolar seesaw concept is qualitatively analogous to that of (*9*) in that it implies the existence of a heat reservoir which convolves the northern signal, producing a southern signal with a longer characteristic timescale. Our approach is slightly different in that we relate the rate of Antarctic temperature change directly to the northern temperature anomaly. Indeed, we note that for some long stadial events, particularly those associated with glacial terminations, Antarctic temperatures appear to rise unabated until an abrupt warming event occurs in the north (*19*). On the other hand our formulation does not imply that Antarctic temperatures must continue to rise indefinitely whenever Greenland is cold, only while it is cold with respect to background conditions (defined by the orbital-timescale component). We also note that northern temperature (regardless of background conditions) is not always constant throughout stadial events. For example, Greenland warmed significantly during cold stadial 21 (Fig. 2D). By our formulation, the rate of Antarctic temperature rise during this event would decrease correspondingly, in line with observations (Fig. 2A) (*20*).

We employ a thresholding approach for predicting the occurrence of abrupt Greenland warming events based on minima in the second time differential of AA_T (AA_T'') (Fig. 2E, F). This has an advantage over use of the first differential (decreasing through zero) because it is capable of distinguishing between events of varying magnitude and incorporates information about conditions before and after an abrupt event (*6*). Using a relatively insensitive threshold (blue dashed line in Fig. 2F) we are able to identify the largest D-O temperature shifts recorded in Greenland while 'smaller' events, such as D-O 2, require a more sensitive threshold (red line). Based on this we are able to identify almost all of the canonical D-O events over the last 90 kyr without introducing 'spurious events'. We incorporate a correction, based on the time integrated per 55cm sample of ice (*7*), to account for loss of temporal resolution in the deeper parts of the ice core (*6*).

Our synthetic reconstruction of Greenland temperature closely resembles the observed record both in terms of its timing and the structure of individual events (Fig. 2). This is despite probable variability in the relationships between $\delta^{18}O$ (for GISP2) or δD (for EDC) versus local temperature through time (*21*) and other millennial-scale variability that might not be related to the bipolar seesaw. We find similar results using alternative Antarctic ice core records (*6*). Based on the predictive ability of GL_T_syn over the last ~100 kyr we extend our reconstruction back to ~800 ka (Figs. 3, 4). In doing so we implicitly assume that the empirical relationships observed over the last glacial cycle held during earlier periods. Given the inherent uncertainty in this assumption we do not make a claim for significant skill at predicting the absolute amplitude of earlier events but we do suggest that, to the extent that the underlying physical mechanisms indeed persisted throughout the last 800 kyr, the timing and overall structure of events will be relatively robust.

In order to test this hypothesis we compare our synthetic reconstructions with real climate records. The record of Asian monsoon variability derived from cave deposits (speleothems) in China (*5, 22*) is one of the best candidates for this task (Fig. 3). The Chinese speleothem $\delta^{18}O$ record is thought to represent changes in the proportion of low $\delta^{18}O$ (summer monsoon) rainfall within annual totals (*22*) and can be considered a measure of the amount of summer monsoon rainfall or monsoon intensity. The combined record from several deposits taken from a number of caves provides a continuous, absolutely-dated record over the last ~400 kyr (*22*). The record is dominated by orbital-timescale changes, possibly related to the influence of boreal summer insolation on the strength of the Asian monsoon (*6*). Removal of this variability by normalising to the insolation curve (*6*) reveals a significant component of millennial-timescale activity which has been shown to correspond with D-O variability over Greenland during the last glacial cycle (*5, 22*). This correspondence is thought to be caused by latitudinal shifts in the position of the Intertropical Convergence Zone (ITCZ) and related atmospheric phenomena, in response to variations in the AMOC and related changes in North Atlantic temperature (*11*).

There is a strong one-to-one correspondence between inferred weak-monsoon events and our reconstructed cold events in Greenland (Fig. 3). Moreover, there are pronounced similarities in the structure of abrupt events, particularly during deglacial episodes (terminations); the multiple weak-monsoon events associated with glacial terminations of the Late Pleistocene (*22*) are reflected by multiple cold events in our records. Our reconstruction suggests the occurrence of large amplitude 'D-O-type' oscillations between 160-180 ka (during MIS 6; Fig. 3). These may be compared with similar events in the records of planktonic $\delta^{18}O$ and tree pollen from a marine sediment core taken from the Iberian Margin (*23*). Based on the findings of Shackleton *et al.* (*24*) the Iberian Margin records were tuned to the EDC δD record via the record of benthic $\delta^{18}O$ from the same core (*23*). The tuning exercise did not involve the surface records, which therefore provide a quasi-objective 'target' for comparing with our reconstruction (which should be aligned with the surface-ocean records according to (*24*)) and we note there is good agreement in the timing and structure of the abrupt events during MIS 6. We also note good agreement between our reconstructions and the record of atmospheric CH_4 (*25*). Our predicted D-O warming events are generally aligned with sharp increases in CH_4 (similar to the observed relationship during MIS 3). This relationship holds for the entire 800,000 year record (Fig. 4) and provides critical ground-truthing for our reconstruction.

Building on previous studies (*22*) we employ the precise and absolutely-dated Chinese speleothem record to place our reconstruction on an absolute timescale for the last 400 kyr. We do this by aligning the cold events in our reconstruction with the inferred weak monsoon events in the speleothem record (Fig. 4) (*6*). The EDC3 age scale (which remains the fundamental basis for our model) was derived through a combination of ice flow modelling and various age markers, including orbital tuning constraints (*26*). By tuning the millennial-scale features of GL_T_syn to the speleothem record we provide a refinement of the age scale that provides an alternative to the ultimate dependence on orbital tuning. In addition to providing an absolute timescale for the ice and gas records from Antarctica, we can also use our absolutely-dated Greenland reconstruction as a tuning target for other high-resolution paleo-records (Fig. 4). Here we show the records of ice rafted debris (IRD) from a North Atlantic sediment core (ODP 980) (*4*) and a record of sea surface temperature (SST) from a core off the Iberian Margin (*27*). Each of these records has been tuned to our reconstruction on its absolute timescale (*6*).

Our synthetic records confirm that millennial-timescale variability and abrupt climate oscillations occurred in Greenland throughout the last 800 kyr and more specifically they suggest that the underlying physical mechanisms represented by the conceptual thermal bipolar seesaw were relatively invariant throughout this period. In line with observations for the last glacial period (*28*) our reconstructions suggest that higher amplitude variability and more frequent D-O-like warming events occurred when climate was in an intermediate state or during the transitions between states (Fig. 4). Extending the observations of (*22*) we find that glacial terminations of the Middle to Late Pleistocene in general were characterised by (multiple) oscillations of the bipolar seesaw. This apparently ubiquitous association of millennial-scale climate variability with glacial terminations raises an important question: is this mode of variability a necessary component of deglacial climate change or merely a complicating factor? Previous studies (*28, 29*) have suggested that DO-type variability might represent an inherent resonance of the climate system, attaining significant amplitude only within certain windows of opportunity *i.e.* intermediate climate states. Given that global climate must pass through such a window during deglaciation, one could argued that terminal oscillations of the bipolar seesaw are merely an artefact of deglacial climate change (*29*). However, the precise correspondence observed between bipolar seesaw oscillations and changes in atmospheric CO_2 during glacial terminations (Fig. 4) suggests that the bipolar seesaw may play more than just a passive role in the mechanism of deglaciation *i.e.* through the positive feedbacks associated with increasing CO_2 (*14, 19, 22*). With the supercritical size of continental ice sheets as a possible precondition (*30*), and in combination with the right insolation forcing (*31*) and ice albedo feedbacks, the CO_2 rise associated with an oscillation of the bipolar seesaw could provide the necessary additional forcing to promote deglaciation. In this sense the overall mechanism of glacial termination during the Middle to Late Pleistocene might be viewed as the timely and necessary interaction between millennial- and orbital-timescale variations.

Acknowledgements

We thank the authors of all of the studies cited here for making their results available for this work. This work was supported by a Philip Leverhulme Prize to SB. Additional support was from NERC (UK) awards NE/F002734/1 and NE/G004021/1 to SB, and NSF (US) grants 0502535 and 1103403 to RLE. This study is also part of the British Antarctic Survey Polar Science for Planet Earth Programme, funded by the Natural Environment Research Council (UK).

References and Notes

1. W. Dansgaard *et al.*, A new Greenland deep ice core. *Science* **218**, 1273 (1982).
2. M. Stuiver, P. M. Grootes, GISP2 oxygen isotope ratios. *Quat. Res.* **53**, 277 (2000).
3. G. Bond *et al.*, Correlations between climate records from North-Atlantic sediments and Greenland ice. *Nature* **365**, 143 (1993).
4. J. F. McManus, D. W. Oppo, J. L. Cullen, A 0.5-million-year record of millennial-scale climate variability in the North Atlantic. *Science* **283**, 971 (1999).
5. Y. J. Wang *et al.*, Millennial- and orbital-scale changes in the East Asian monsoon over the past 224,000 years. *Nature* **451**, 1090 (2008).
6. Materials and methods are available as supporting material on Science Online.
7. J. Jouzel *et al.*, Orbital and millennial Antarctic climate variability over the past 800,000 years. *Science* **317**, 793 (2007).
8. W. S. Broecker, Paleocean circulation during the last deglaciation: A bipolar seesaw? *Paleoceanography* **13**, 119 (1998).
9. T. F. Stocker, S. J. Johnsen, A minimum thermodynamic model for the bipolar seesaw. *Paleoceanography* **18**, (2003).
10. K. E. Trenberth, J. M. Caron, Estimates of meridional atmosphere and ocean heat transports. *J. Clim.* **14**, 3433 (2001).
11. M. Vellinga, R. A. Wood, Global climatic impacts of a collapse of the Atlantic thermohaline circulation. *Clim. Change* **54**, 251 (2002).
12. J. C. H. Chiang, M. Biasutti, D. S. Battisti, Sensitivity of the Atlantic Intertropical Convergence Zone to Last Glacial Maximum boundary conditions. *Paleoceanography* **18**, (2003).
13. R. F. Anderson *et al.*, Wind-driven upwelling in the Southern Ocean and the deglacial rise in atmospheric CO_2. *Science* **323**, 1443 (2009).
14. S. Barker *et al.*, Interhemispheric Atlantic seesaw response during the last deglaciation. *Nature* **457**, 1097 (2009).
15. A. Schmittner, O. A. Saenko, A. J. Weaver, Coupling of the hemispheres in observations and simulations of glacial climate change. *Quat. Sci. Rev.* **22**, 659 (2003).
16. E. J. Steig, R. B. Alley, Phase relationships between Antarctic and Greenland climate records. *Annals of Glaciology* **35**, 451 (2002).
17. T. Blunier, E. J. Brook, Timing of millennial-scale climate change in Antarctica and Greenland during the last glacial period. *Science* **291**, 109 (2001).
18. M. Siddall *et al.*, Using a maximum simplicity paleoclimate model to simulate millennial variability during the last four glacial periods. *Quat. Sci. Rev.* **25**, 3185 (2006).
19. E. W. Wolff, H. Fischer, R. Rothlisberger, Glacial terminations as southern warmings without northern control. *Nature Geoscience* **2**, 206 (2009).
20. E. Capron *et al.*, Synchronising EDML and NorthGRIP ice cores using $\delta^{18}O$ of atmospheric oxygen ($\delta^{18}O_{atm}$) and CH_4 measurements over MIS5 (80-123 kyr). *Quat. Sci. Rev.* **29**, 222 (2010).
21. E. Capron *et al.*, Millennial and sub-millennial scale climatic variations recorded in polar ice cores over the last glacial period. *Climate of the Past* **6**, 345 (2010).
22. H. Cheng *et al.*, Ice Age Terminations. *Science* **326**, 248 (2009).
23. V. Margari *et al.*, The nature of millennial-scale climate variability during the past two glacial periods. *Nature Geoscience* **3**, 127 (2010).
24. N. J. Shackleton, M. A. Hall, E. Vincent, Phase relationships between millennial-scale events 64,000- 24,000 years ago. *Paleoceanography* **15**, 565 (2000).
25. L. Loulergue *et al.*, Orbital and millennial-scale features of atmospheric CH4 over the past 800,000 years. *Nature* **453**, 383 (2008).
26. F. Parrenin *et al.*, The EDC3 chronology for the EPICA dome C ice core. *Climate of the Past* **3**, 485 (2007).

27. B. Martrat *et al.*, Four climate cycles of recurring deep and surface water destabilizations on the Iberian margin. *Science* **317**, 502 (2007).
28. M. Schulz, W. H. Berger, M. Sarnthein, P. M. Grootes, Amplitude variations of 1470-year climate oscillations during the last 100,000 years linked to fluctuations of continental ice mass. *Geophys. Res. Lett.* **26**, 3385 (1999).
29. A. Sima, A. Paul, M. Schulz, The Younger Dryas - an intrinsic feature of late Pleistocene climate change at millennial timescales. *Earth Planet. Sci. Lett.* **222**, 741 (2004).
30. M. E. Raymo, The timing of major climate terminations. *Paleoceanography* **12**, 577 (1997).
31. J. D. Hays, J. Imbrie, N. J. Shackleton, Variations in the Earth's orbit: Pacemaker of the Ice Ages. *Science* **194**, 1121 (1976).
32. M. F. Sanchez Goni, F. Eynaud, J. L. Turon, N. J. Shackleton, High resolution palynological record off the Iberian margin: direct land-sea correlation for the Last Interglacial complex. *Earth Planet. Sci. Lett.* **171**, 123 (1999).
33. D. Luthi *et al.*, High-resolution carbon dioxide concentration record 650,000-800,000 years before present. *Nature* **453**, 379 (2008).
34. L. E. Lisiecki, M. E. Raymo, A Pliocene-Pleistocene stack of 57 globally distributed benthic $\delta^{18}O$ records. *Paleoceanography* **20**, PA1003 (2005).

Supporting Online Material

www.sciencemag.org

Materials and Methods

Figs. S1-S14

References (S1-S35)

Tables S1-S3

Figure Annotations

Figure 1. Ice core records from Greenland (GISP2) and Antarctica (EDC) (all records have orbital-timescale variability removed). (A) Methane (*17, 25*) with tuning points (crosses) used to place all records on the EDC3 age model (*26*), Greenland temperature (GL_T_hi with 200 yr smooth) derived from $\delta^{18}O$ of ice (*2*) and Antarctic temperature (AA_T_hi, 200 yr smooth) from δD of ice (*7*). First derivatives of AA_T_hi (AA_T_hi') are shown for various smoothing lengths (in brackets) of the undifferentiated record. (B) Lead/lag correlation of the methane records suggests successful tuning of the gas records. (C) Lead/lag correlations between GL_T_hi, AA_T_hi and AA_T_hi' reveal the well-known relation between northern and southern temperature records and the antiphase relationship between GL_T_hi and AA_T_hi'.

Figure 2. Reconstructing millennial-scale climate variability over Greenland using the Antarctic temperature record. (A) The record of δD from the EDC ice core (AA_T) (*7*) with a 7000 yr smooth of the same record (AA_T_lo). (B) Removal of orbital-timescale variability and application of a 700 yr smooth (*6*) produces AA_T_hi. (C) AA_T_hi is differentiated and then scaled to GL_T_hi (green curve) to produce GL_T_syn_hi (orange curve). (D) A synthetic reconstruction of Greenland temperature variability (GL_T_syn; red curve) constructed by adding GL_T_syn_hi to GL_T_syn_lo (*6*). Green curve is GISP2 $\delta^{18}O$ placed on EDC3 via methane tuning (Fig. 1). (F) Minima in AA_T'' below a threshold (dashed lines) are employed to predict the occurrence of major warming events in Greenland, identified by the corresponding coloured dots in (E). A threshold value of -1.2×10^{-5} (red dashed line and dots) has good success at picking canonical D-O events (green numbers in (D) and (E)) without introducing spurious events.

Figure 3. Comparison of reconstructed Greenland climate variability with other records. The normalised record of monsoon variability from China (A) (*5, 22*), marine records from the Iberian

Margin (C) (*32*), (D, E) (*23*) and the record of atmospheric CH_4 (G) (*25*) share many features in common with our records derived from the Antarctic temperature record (B, F). Coloured dots in (H) represent the occurrence of D-O events predicted from AA_T'' using a fixed (red) or variable (blue) threshold (*6*). All records are on the EDC3 timescale (*26*) except the monsoon record which is on its own absolute timescale (*22*). The pollen record from MD95-2042 (*32*) (C) was placed on EDC3 by tuning the corresponding planktonic $\delta^{18}O$ record (*24*) to GL_T_recon. Grey bars indicate cold conditions and periods of weak monsoon. Glacial terminations are indicated by Roman numerals.

Figure 4. 800,000 years of abrupt climate variability. Records of North Atlantic IRD (*4*), monsoon rainfall (*5, 22*) (normalised) and SST from the Iberian Margin (*27*) all show strong similarities with our reconstruction of Greenland climate variability (GL_T_syn_hi and GL_T_syn). Glacial Terminations (identified by Roman numerals) are characterised by cold conditions across Greenland and the North Atlantic and weakened monsoon rainfall, with a corresponding rise in atmospheric CO_2 (*33*), followed by an abrupt warming over Greenland, strengthening of the monsoon and sharp rise in atmospheric CH_4 (*25*). Pink boxes indicate terminal Northern Hemisphere cold periods. Red and blue dots are predicted D-O warming events using a fixed or variable threshold respectively. Lowermost curves in each panel are moving windows of the standard deviation of AA_T_hi' (note that orbital-timescale variations have been removed; blue is 5kyr, green is 10kyr window). All records are on the new Speleo-Age (Panel A) or the EDC3 (Panel B) timescale except the benthic $\delta^{18}O$ stack (LR04) of (*34*), which is on its own timescale. Increased millennial-scale activity is generally observed during transitions between climate states with minimal activity during interglacials and glacial maxima.

EMBARGOED UNTIL 2:00 PM US ET THURSDAY, 8 SEPTEMBER 2011

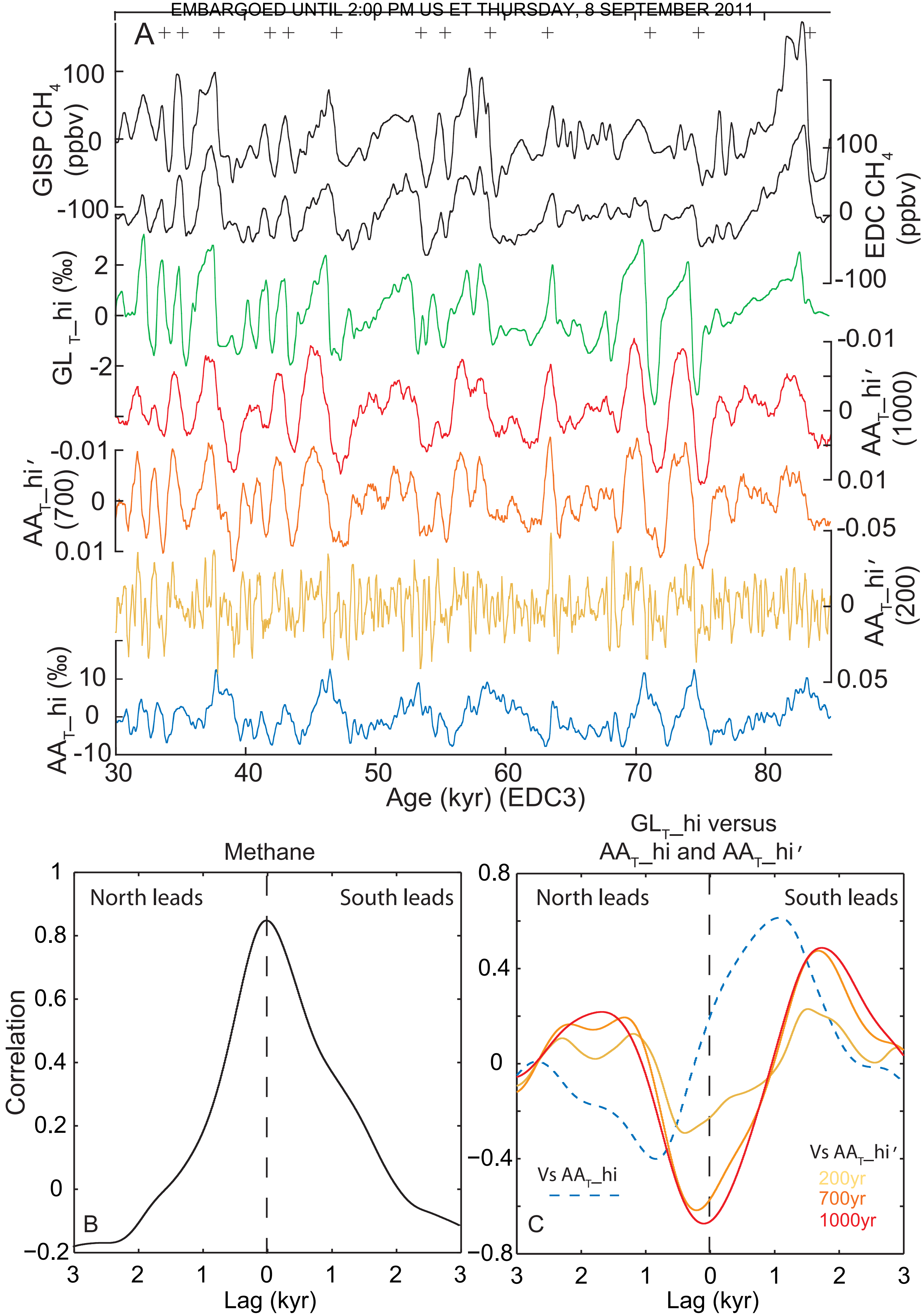

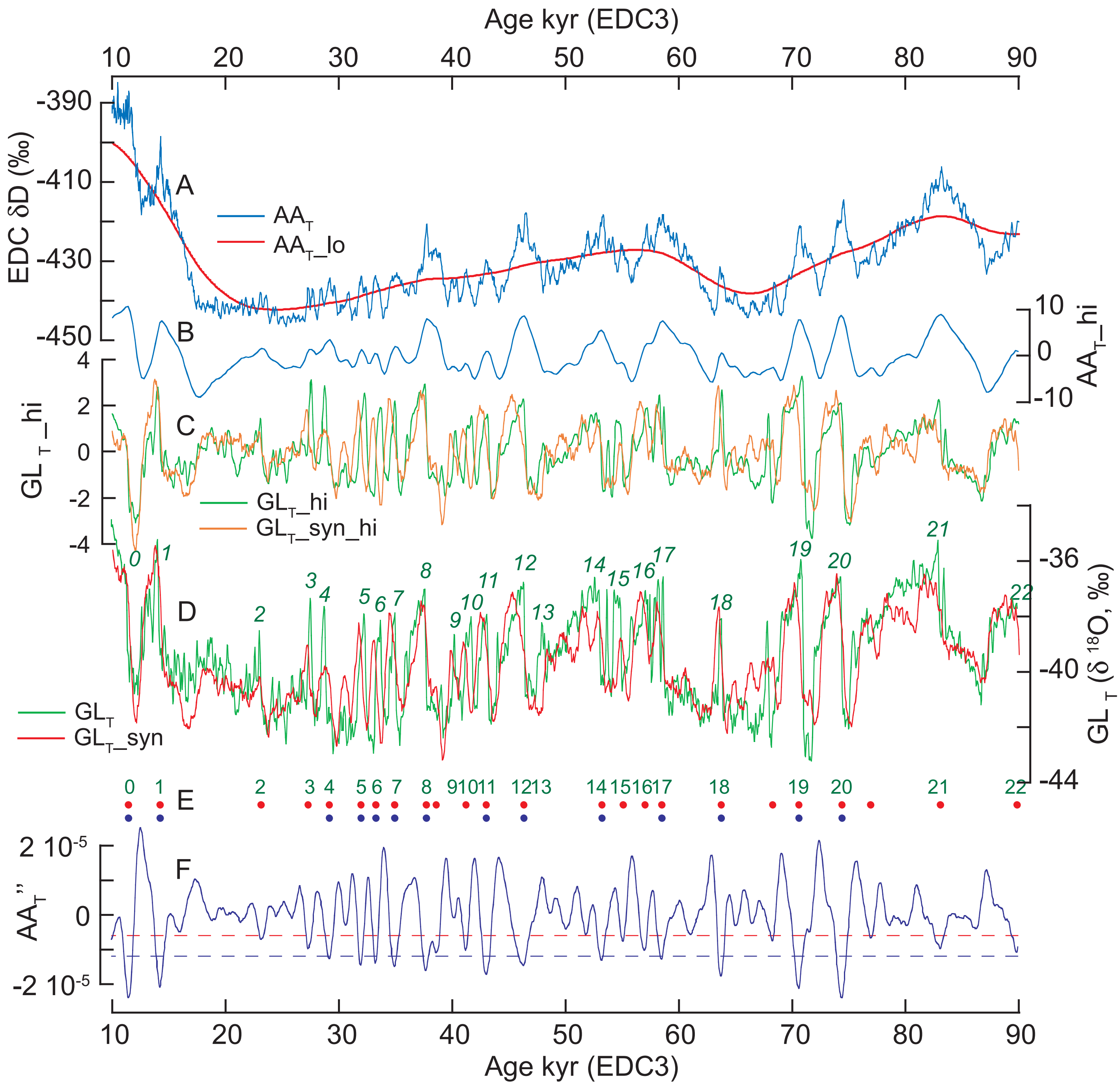

Age kyr (EDC3)
10 20 30 40 50 60 70 80 90
EDC δD (‰)
-390 -410 -430 -450
A
AA_T
AA_T_lo
B
AA_T_hi
10 0 -10
C
GL_T_hi
4 2 0 -2 -4
GL_T_hi
GL_T_syn_hi
D
GL_T (δ 18O, ‰)
-36 -40 -44
GL_T
GL_T_syn
0 1 2 3 4 5 6 7 8 9 10 11 12 13 14 15 16 17 18 19 20 21 22
E
F
AA_T''
2 10-5
0
-2 10-5
10 20 30 40 50 60 70 80 90
Age kyr (EDC3)

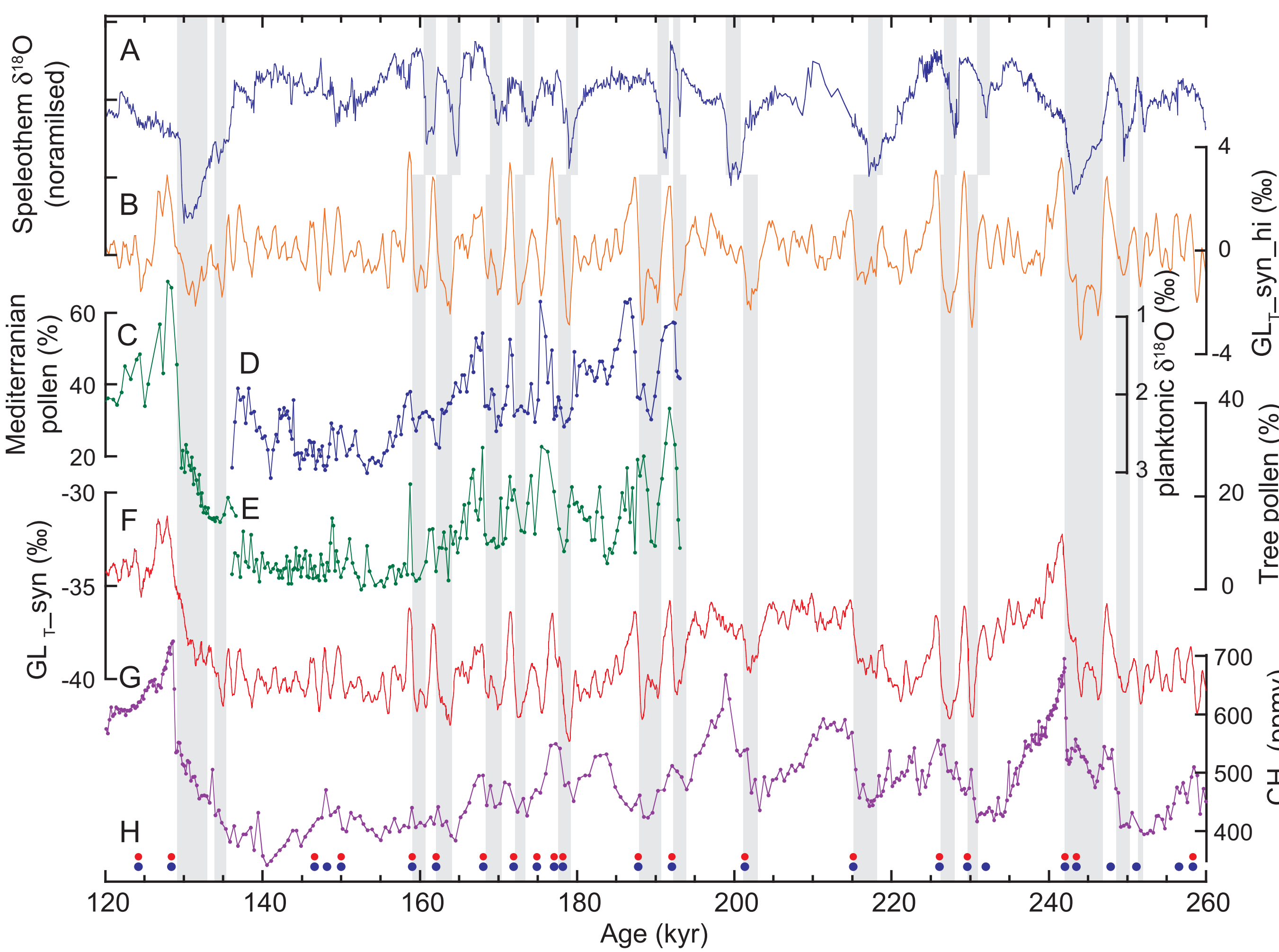

Speleothem δ18O (noramilsed)
A
B
GLT_syn_hi (‰)
4
0
-4
Mediterranian pollen (%)
60
40
20
C
D
planktonic δ18O (‰)
1
2
3
Tree pollen (%)
40
20
0
-30
F
E
GL T_syn (‰)
-35
-40
G
CH4 (ppmv)
700
600
500
400
H
120
140
160
180
200
220
240
260
Age (kyr)

EMBARGOED UNTIL 2:00 PM US ET THURSDAY, 8 SEPTEMBER 2011

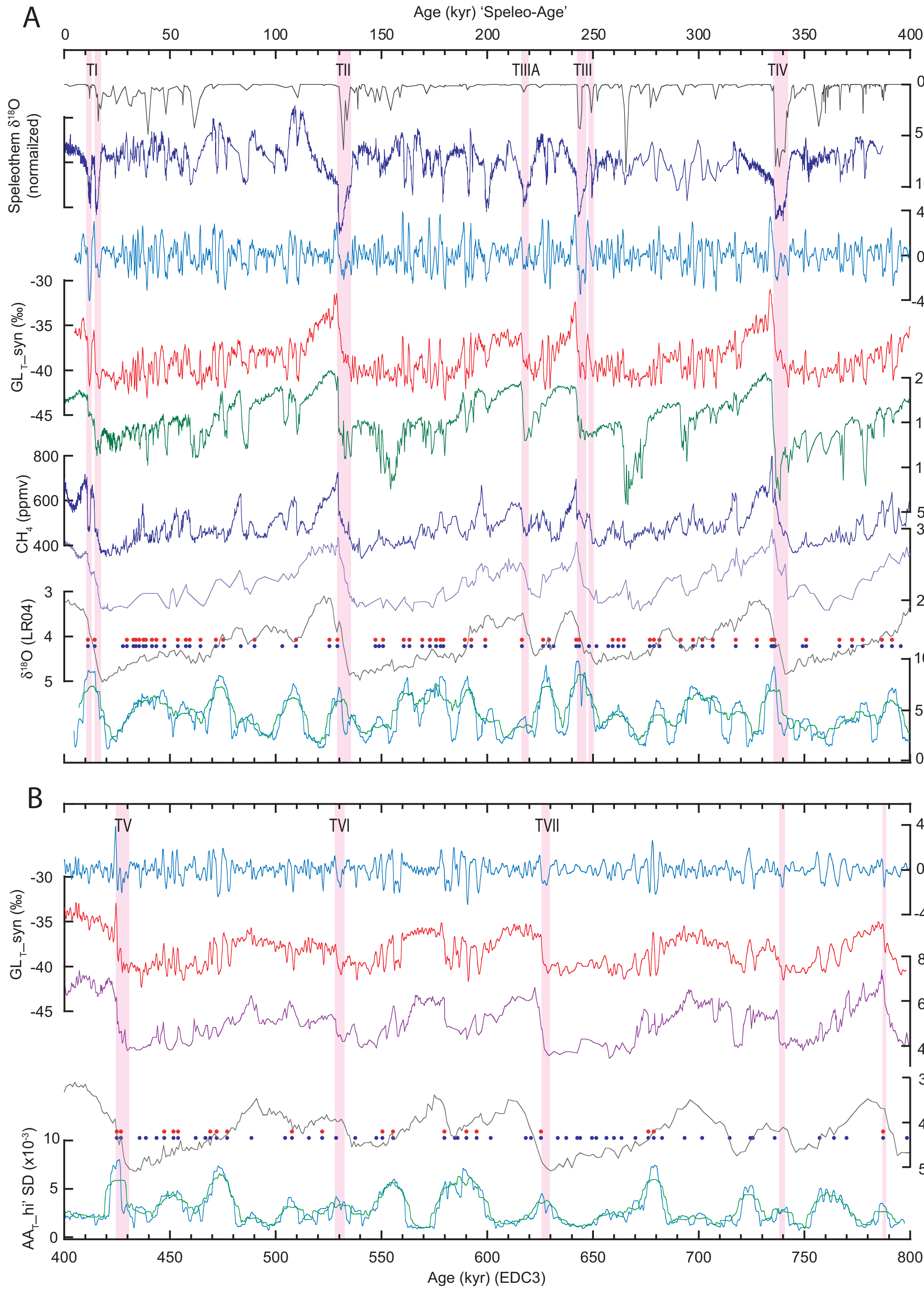

800,000 years of abrupt climate variability

Stephen Barker, Gregor Knorr, R. Lawrence Edwards, Frédéric Parrenin, Aaron E. Putnam, Luke C. Skinner, Eric Wolff and Martin Ziegler

Supporting Online Material

The US National Research Council Committee on Abrupt Climate Change (*1*) defines an abrupt climate change as one that occurs when the climate system is forced to cross some threshold, triggering a transition to a new state at a rate determined by the climate system itself and faster than the cause.

Smoothing records and removing orbital-timescale variability

All smoothing is performed by a applying a running mean (of the length specified) twice to the evenly sampled datasets. Removal of orbital-timescale variability is achieved by subtracting a 7 kyr smooth.

Smoothing of the Antarctic temperature record its derivative

Before taking the first derivative of AA_T we remove orbital-timescale variability to give AA_T_hi, in order to remove ambiguities resulting from the superposition of millennial-scale events on orbital-timescale variations (Fig. S1). Since the changes we are interested in (abrupt warming events in Greenland) appear as short-lived minima in the record of AA_T'' we do not need to apply this treatment to the original temperature record (even before taking the first differential) for deriving the second differential. This is demonstrated by the similarity between the records of AA_T'' with and without removal of the 7 kyr smooth (Fig. S1). Although it makes little difference we choose not to remove orbital-timescale variability before deriving the second differential in order to minimise the number of processing steps involved in our analysis.

The act of differentiating (by finite differences) amplifies noise in the original record and it is therefore necessary to smooth this record before differentiating. However, the choice of smoothing window length is a trade-off between loss of unwanted noise and loss in the signal we wish to isolate. These effects can be observed by comparing records of AA_T_hi' produced after smoothing AA_T with various window lengths, and their correlation with GL_T_hi (Fig. S2). We suggest that a smoothing window of 700 years provides a reasonable compromise between noise reduction and signal fidelity. This is comparable to the running mean window applied by the study of (*2*).

Selecting events when the first derivative (AA_T_hi') decreases through zero (which would coincide with abrupt warming events in Greenland, according to the seesaw model) provides another means to assess the effect of different smoothing window length (Fig. S3). We note that low order smoothing (200-300 yr) predicts many events that do not have obvious correlatives in Greenland while high order (1000 yr) smoothing results in loss of events. We also smooth the record of AA_T' before differentiating a second time in order to analyse minima in AA_T'' (Fig. S3). Critically we note that the timing of significant minima in AA_T'' (used to identify D-O warming events) is not particularly sensitive to the choice of filter length. We apply a 700 yr smooth to AA_T' before differentiating a second time to produce AA_T''. We note that a longer smoothing window results in loss of events.

GL_T versus AA_T' and the effect of uncertainty in Δage

In order to compare the phasing between temperature records from Greenland and Antarctica we rely on the methane tuning method developed by Blunier and Brook (*3, 4*). By making the assumption that changes in atmospheric CH_4 will be essentially contemporaneous in both hemispheres it is possible to place the gas records from disparate locations on a common timescale. In order to place the corresponding temperature records (which are most commonly derived from the ice phase) on the same common timescale, it is necessary to know the age offset (Δage) between the ice and trapped gas at any depth within the core (the gas will always be younger the surrounding ice because the circulation of gas within the firn is only stopped once the ice is compacted). Unfortunately the uncertainty in the age offset is considerable (up to hundreds of years). Therefore we are unable to determine the precise phase relationships between the records derived from ice to better than ~200 years based on this method. As shown in the main text Figure 1, the approximate out-of-phase relationship between GL_T_hi and AA_T_hi' actually suggests a small (100-150 yr) lead of Greenland over Antarctica. However, when we perform the same analysis on the GISP (Greenland) and Byrd (Antarctica) temperature records (as aligned by (*4*)) we find that AA_T_hi' leads GL_T_hi by ~200 years (Fig. S4). We suggest that these differences result from the uncertainties in Δage and argue that the true relationship should be antiphase. Our findings appear to resolve the discussion between (*5*), (*6*) and (*7*) who were essentially describing the differences between GL_T_hi versus AA_T_hi and GL_T_hi versus AA_T_hi'.

Construction of "GL_T_syn"

To produce a reconstruction of Greenland temperature variability (Fig. S5) from the EDC δD record (*8*) we first apply a 7000 year smooth to the Antarctic record to produce AA_T_lo. We then subtract AA_T_lo from AA_T and smooth the result at 700 year to produce AA_T_hi. This is differentiated to produce AA_T_hi'. We then normalise AA_T_hi' (divide through by its own standard deviation) and scale it to the record of GL_T_hi by multiplying the normalised record of AA_T_hi' by the standard deviation of GL_T_hi. This produces GL_T_syn_hi. We produce GL_T_syn_lo by scaling the record of AA_T_lo to GL_T_lo (by normalising and applying the same mean and standard deviation) and shifting it towards younger ages by 2000 years (see next paragraph). GL_T_syn is then the sum of GL_T_syn_hi and GL_T_syn_lo.

The thermal bipolar seesaw model was constructed to explain millennial-scale oscillations during the last glacial period. However, the temperature records from Greenland ice cores include longer-term variations (so-called orbital-timescale variability). We wish to produce a reconstruction of what Greenland temperature records might look like if they extended back as far as those from Antarctica. This requires us to add orbital-timescale variability to our record of GL_T_syn_hi. The orbital-timescale component of the Antarctic temperature record (AA_T_lo) is highly correlated with GL_T_lo over the last 100 kyr (*9*) (Figs. S5, S6). Furthermore, both signals appear correlated to variations in northern hemisphere summer insolation (*10-13*). While the link between the northern temperature record and northern summer insolation may be comparatively straightforward (through direct effects such as ice albedo), the correlation between northern summer insolation and southern temperature records is less obvious (*13*). Explanations have most often argued that northern hemisphere insolation must provide an indirect forcing on southern hemisphere temperatures (through *e.g.* CO_2 or ocean circulation changes) (*14, 15*) although a recent study suggests that southern insolation itself may be responsible via the influence of summer duration (which is in phase with northern hemisphere summer intensity) as opposed to intensity (*12*). Whatever the explanation, the correlation holds for at least the last 800,000 years (*8*). Atmospheric CO_2 concentrations may also play a role in the interhemispheric symmetry of the temperature records on longer timescales. Although changes in CO_2 typically lag temperature changes over Antarctica by several hundreds of years on multi-millennial timescales (*16*) CO_2 probably plays a role in the amplitude of these changes (for example it may help to explain the amplitude of glacial-interglacial changes). Given the observed similarity between the low frequency components of the Greenland and Antarctic records over the last 100 kyr, we suggest that the record of AA_T_lo represents a reasonable substitute for GL_T_lo in our reconstruction of Greenland temperature variability.

The record of AA_T_lo appears to lead that of GL_T_lo by around 2000 years (*9*) although the precise lag is difficult to determine given the length of the records (Figs. S5, S6). This may be due to *e.g.* the slow response of northern hemisphere ice sheets to insolation forcing or it may reflect the pervasive influence of millennial-scale oscillations on the Antarctic record (for example during late MIS 4 (HS6), when Greenland was cold, Antarctica warmed, possibly through the seesaw mechanism. This would give rise to an apparent lead of Antarctic over Greenland on longer timescales). When the record of AA_T_lo is scaled to GL_T_lo (same mean and standard deviation) the offset between the two records (Fig. S5F) is typically less than 1‰. This offset can be reduced by shifting GL_T_syn_lo by 2000 years to provide a better match with GL_T_lo. The offset is relatively small compared to the high amplitude of D-O oscillations (typically 3-4‰) and to the overall magnitude of glacial-interglacial variability. Furthermore the offset changes slowly with respect to the abruptness of D-O events. We therefore include a shift of 2000 years in GL_T_syn_lo. When we include GL_T_syn_lo in our reconstruction of GL_T_syn we achieve a reasonable result (Fig. 2G).

We chose the EDC δD record for our construction of GL_T_syn because it is the longest published record and we compared our results with the GISP ice core because this allows straightforward derivation a common age scale via CH_4 tuning (Fig. 1). For completeness we show a comparison of the first differentials of EDC, EDML (both normalised) and a composite Antarctic record (derived by tuning and normalising the isotope records from EDC (*8*), EDML (*17*), Vostok (*11*), Dome Fuji (*18*) and Byrd (*19*)) with the millennial-scale components of the GISP (*20*) and NGRIP (*21*) ice cores (Fig. S7).

Synthetic records are given in Table S2.

Prediction of 'D-O-type' events using the Antarctic record

We employ a thresholding approach for predicting the occurrence of abrupt Greenland warming events based on minima in the second time differential of AA_T (AA_T'') (Fig. 2E, F). This has an advantage over use of the first differential (decreasing through zero) because it is capable of distinguishing between events of varying magnitude and incorporates information about conditions before and after an abrupt event. For example, the large D-O events, 19 and 20, were characterised by a rapid transition from pronounced warming to equally pronounced cooling over Antarctica (Fig. 2). This information is captured by the exaggerated minima in AA_T'', which may then reflect particularly significant changes in the AMOC and related atmospheric phenomena associated with these events. If a minimum in AA_T'' exceeds a threshold, an event is generated and assigned the age of that minimum (Fig. 2E). Using a relatively insensitive threshold (blue dashed line in Fig. 2F) we are able to identify the largest D-O temperature shifts recorded in Greenland while 'smaller' events, such as D-O 2, require a more sensitive threshold (red line). Based on this we are able to identify almost all of the canonical D-O events over the last 90 kyr without introducing 'spurious events'.

Correcting for signal loss due to sample time integration

Before applying our two approaches for reconstructing Greenland climate to the full 800 kyr record of AA_T (*i.e.* δD) from the EDC ice core we need to investigate the possible effects of ice flow and diffusion in the deeper parts of the record. Both of these processes may result in a reduction in the amplitude of variability in δD (either through diffusion (*22, 23*)) or simply because the sampling for δD measurements (made on 55cm sections of ice) tends to integrate longer time intervals for deeper parts of the core. For example, within the upper few meters of the EDC ice core each 55cm sample represents < 10 years of ice accumulation whereas at 3042m (~640 ka) a 55cm sample integrates >1350 years of ice (Fig. S8a). It has also recently been argued that diffusion length scales may reach up to 40cm for the deepest parts of the EDC ice core (*23*). Since this is of the same order as the sampling window we address both issues together. We do so by constructing a synthetic Antarctic ice core temperature record ($SynAA_T$) (Fig. S8) and use this to investigate the potential effects of fidelity loss in deeper parts of the record. We start by assuming that the real EDC ice core temperature record for the last 100 kyr or so represents actual temperature variations over Antarctica (*i.e.* without significant signal attenuation on millennial-timescales). We then select a 100 kyr interval with similar δD values at either end (in this case ~12 to ~112 ka) and produce a synthetic history of temperature for 800 kyr by repeating this interval 8 times. Finally we 'sample' this synthetic temperature history in the same manner as the actual EDC ice core record samples the real temperature history over Antarctica (by integrating the same time intervals as each 55cm sample does for the real record).

The loss of signal amplitude is immediately apparent for deeper sections of the synthetic record (Fig. S8A). The corresponding 'loss' of predicted D-O events, based on minima in AA_T'' below a fixed threshold, is significant. We address this by allowing the picking threshold to vary according to the time integrated by each 55cm of ice (Fig. S8A). We apply the simplest approach for incorporating the 'time-per-sample' factor into our D-O prediction algorithm. For adjusting the threshold used to pick D-O events based on minima in AA_T'', we ratio the corresponding time-per-sample to the minimum value for this parameter (5.81 yr), scale it (divide by 2.3×10^7) and add it to a baseline threshold (-1×10^{-5}) (Fig. S8A, B). This operation effectively accounts for smoothing of the record by exaggerating the minima in AA_T'' with respect to the threshold. Use of the variable threshold recovers most of the D-O events that were lost using the fixed threshold approach (Fig. S8C). The choice of parameters for the thresholding exercise was based on a trade-off between picking as many canonical D-O events as possible while minimising the number of predicted events with no obvious analogy in Greenland. Thus some canonical events are not picked (*e.g.* events 2 and 9). We note that for sections of the record where the time-integrated-per-sample approaches or exceeds 1000 years (~600-800 ka) two individual millennial-scale events may be merged into a single event, which our variable threshold cannot account for. Therefore, while we are confident that our approach does not predict a significant number of spurious events, we must acknowledge that some events may be lost altogether.

We could use a similar approach to adjust the amplitude of variability observed in the record of AA_T_hi' (and therefore in $GL_T\_syn\_hi$). However, the long-lived nature of some Antarctic warming and cooling events (especially those associated with glacial terminals) means that in these cases the increase in sample time integration does not impact the first differential to a significant degree (Fig. S9). Correcting for signal attenuation would therefore result in a spurious amplification of the AA_T_hi' record in certain places and we choose not to apply an adjustment to GL_T_syn. It must be acknowledged therefore that as well as the total loss of very short events, the amplitude of shorter events (~1-2 kyr) in the oldest portion of GL_T_syn (600-800 ka) will be reduced relative to the actual Greenland events they correspond with.

Picked D-O events are given in Table S3.

The Chinese speleothem record

In order to assess the millennial-scale variability within the Chinese speleothem record we need to remove the orbital-scale variations, which mirror July insolation at 65ºN (*24*) (Fig. S10) (we note that there is currently some discussion about the precise insolation target that should be used (*25, 26*) but choose that which is in-phase with the orbitally-filtered speleothem record). We achieve this by removing the normalised (by subtracting its mean and dividing through by its standard deviation) insolation curve from the normalised speleothem record (Fig. S10). Before normalisation, the individual speleothem records require some adjustment to align them to a common scale. This is achieved by subtracting 1.6 from the Hulu Cave records to account for the difference in elevation and location between the various cave sites (*24*).

Derivation of absolute timescales

Thanks to the near one-to-one correspondence between 'weak monsoon events' in the detrended speleothem record and cold events in our synthetic records, GL_T_syn_hi and GL_T_syn (main text Fig. 3) we are able to align these events in order to place the EDC records on the absolute 'Speleo-Age' timescale (Fig. S11A, S12). Uncertainties in resultant age model ('Speleo-Age') arise from uncertainties in the absolute dating of the speleothem record (dating error) and the fact that 'abrupt' transitions in both records (GL_T_syn and speleothem $\delta^{18}O$) sometimes appear to last up to hundreds of years (tuning error). We provide estimates of these errors with their corresponding tie points in Table S1. It is clear that this exercise will improve as more speleothem records are produced and as dating methods improve. For now we do not attempt alignment where the speleothem record has insufficient resolution to allow recognition of abrupt events (*i.e.* the interval 315-265 ka). In general the resultant offset between our absolute timescale for EDC and the published EDC3 age model (*27*) is of the order 0-1000 years with some events shifted by ~3000 yr and up to 5000 yr toward the oldest part of the speleothem record (Table S1). These estimates are within the age uncertainties of the EDC3 age model (*27*). These offsets are also similar in magnitude to our estimate of the total uncertainty in our absolute age model although our revised age model in general shifts the record toward older ages.

Our revised age model for the EDC records is fundamentally based on the EDC3 age model and should be considered a refinement of that. From here we derive absolute timescales for the records from ODP 980 in the North Atlantic (*28*) (Fig. S11B, S13) and MD01-2444 and MD01-2443 from the Iberian Margin (*29*) (Fig. S11C; S14).

We note good correspondence between our absolute age model and the results of Drysdale *et al.* (*30*) for Termination II. We derive an age of 129.6 ± 0.7 ka for the end of Heinrich event 11. This compares with 129 ± 1.5 ka by (*30*).

Supplementary references.

1. National Research Council, Committee on Abrupt Climate Change, *Abrupt Climate Change: Inevitable Surprises*. (The National Academies Press, Washington DC, 2002).
2. B. Stenni *et al.*, The deuterium excess records of EPICA Dome C and Dronning Maud Land ice cores (East Antarctica). *Quat. Sci. Rev.* **29**, 146 (2010).
3. T. Blunier *et al.*, Asynchrony of Antarctic and Greenland climate change during the last glacial period. *Nature* **394**, 739 (1998).
4. T. Blunier, E. J. Brook, Timing of millennial-scale climate change in Antarctica and Greenland during the last glacial period. *Science* **291**, 109 (2001).
5. A. Schmittner, O. A. Saenko, A. J. Weaver, Coupling of the hemispheres in observations and simulations of glacial climate change. *Quat. Sci. Rev.* **22**, 659 (2003).
6. P. Huybers, Comments on 'Coupling of the hemispheres in observations and simulations of glacial climate change' by A. Schmittner, O.A. Saenko, and A.J. Weaver. *Quat. Sci. Rev.* **23**, 207 (2004).
7. A. Schmittner, O. A. Saenko, A. J. Weaver, Response to the comments by Peter Huybers. *Quat. Sci. Rev.* **23**, 210 (2004).
8. J. Jouzel *et al.*, Orbital and millennial Antarctic climate variability over the past 800,000 years. *Science* **317**, 793 (2007).
9. C. Wunsch, Greenland - Antarctic phase relations and millennial time-scale climate fluctuations in the Greenland ice-cores. *Quat. Sci. Rev.* **22**, 1631 (2003).
10. W. Dansgaard *et al.*, Evidence for General Instability of Past Climate from a 250-Kyr Ice-Core Record. *Nature* **364**, 218 (1993).
11. J. R. Petit *et al.*, Climate and atmospheric history of the past 420,000 years from the Vostok ice core, Antarctica. *Nature* **399**, 429 (1999).
12. P. Huybers, G. Denton, Antarctic temperature at orbital timescales controlled by local summer duration. *Nature Geoscience* **1**, 787 (2008).
13. P. Huybers, Antarctica's Orbital Beat. *Science* **325**, 1085 (2009).
14. R. B. Alley, E. J. Brook, S. Anandakrishnan, A northern lead in the orbital band: north-south phasing of Ice-Age events. *Quat. Sci. Rev.* **21**, 431 (2002).
15. J. Imbrie *et al.*, On the structure and origin of major glaciation cycles 2. the 100,000-year cycle. *Paleoceanography* **8**, 699 (1993).
16. J. Ahn, E. Brook, Atmospheric CO_2 and climate from 65 to 30 ka B.P. *Geophys. Res. Lett.* **34**, doi:10.1029/2007/2007GL029551 (2007).
17. EPICA, One-to-one coupling of glacial climate variability in Greenland and Antarctica. *Nature* **444**, 195 (2006).
18. K. Kawamura *et al.*, Northern Hemisphere forcing of climatic cycles in Antarctica over the past 360,000 years. *Nature* **448**, 912 (2007).
19. S. J. Johnsen, H. B. Clausen, Dansgaar.W, C. C. Langway, Oxygen Isotope Profiles through Antarctic and Greenland Ice Sheets. *Nature* **235**, 429 (1972).
20. M. Stuiver, P. M. Grootes, GISP2 oxygen isotope ratios. *Quat. Res.* **53**, 277 (2000).
21. NGRIP_members, High-resolution record of Northern Hemisphere climate extending into the last interglacial period. *Nature* **431**, 147 (2004).
22. S. J. Johnsen, Stable isotope homogenization of polar firn and ice. in *Isotopes and Impurities in Snow and Ice*. (IAHS, Grenoble, 1977), vol. 11B, pp. 210-219.
23. K. Pol *et al.*, New MIS 19 EPICA Dome C high resolution deuterium data: Hints for a problematic preservation of climate variability at sub-millennial scale in the "oldest ice". *Earth Planet. Sci. Lett.* **298**, 95 (2010).
24. Y. J. Wang *et al.*, Millennial- and orbital-scale changes in the East Asian monsoon over the past 224,000 years. *Nature* **451**, 1090 (2008).

25. S. C. Clemens, W. L. Prell, Y. B. Sun, Orbital-scale timing and mechanisms driving Late Pleistocene Indo-Asian summer monsoons: Reinterpreting cave speleothem delta O-18. *Paleoceanography* **25**, (2010).
26. M. Ziegler, E. Tuenter, L. J. Lourens, The precession phase of the boreal summer monsoon as viewed from the eastern Mediterranean (ODP Site 968). *Quat. Sci. Rev.* **29**, 1481 (2010).
27. F. Parrenin *et al.*, The EDC3 chronology for the EPICA dome C ice core. *Climate of the Past* **3**, 485 (2007).
28. J. F. McManus, D. W. Oppo, J. L. Cullen, A 0.5-million-year record of millennial-scale climate variability in the North Atlantic. *Science* **283**, 971 (1999).
29. B. Martrat *et al.*, Four climate cycles of recurring deep and surface water destabilizations on the Iberian margin. *Science* **317**, 502 (2007).
30. R. N. Drysdale *et al.*, Evidence for Obliquity Forcing of Glacial Termination II. *Science* **325**, 1527 (2009).
31. Y. J. Wang *et al.*, A high-resolution absolute-dated Late Pleistocene monsoon record from Hulu Cave, China. *Science* **294**, 2345 (2001).
32. H. Cheng *et al.*, Ice Age Terminations. *Science* **326**, 248 (2009).
33. E. J. Steig, R. B. Alley, Phase relationships between Antarctic and Greenland climate records. *Annals of Glaciology* **35**, 451 (2002).
34. A. Berger, M. F. Loutre, Insolation Values for the Climate of the Last 10 Million Years. *Quat. Sci. Rev.* **10**, 297 (1991).
35. L. E. Lisiecki, M. E. Raymo, A Pliocene-Pleistocene stack of 57 globally distributed benthic δ^{18}O records. *Paleoceanography* **20**, PA1003 (2005).

Supplementary figures

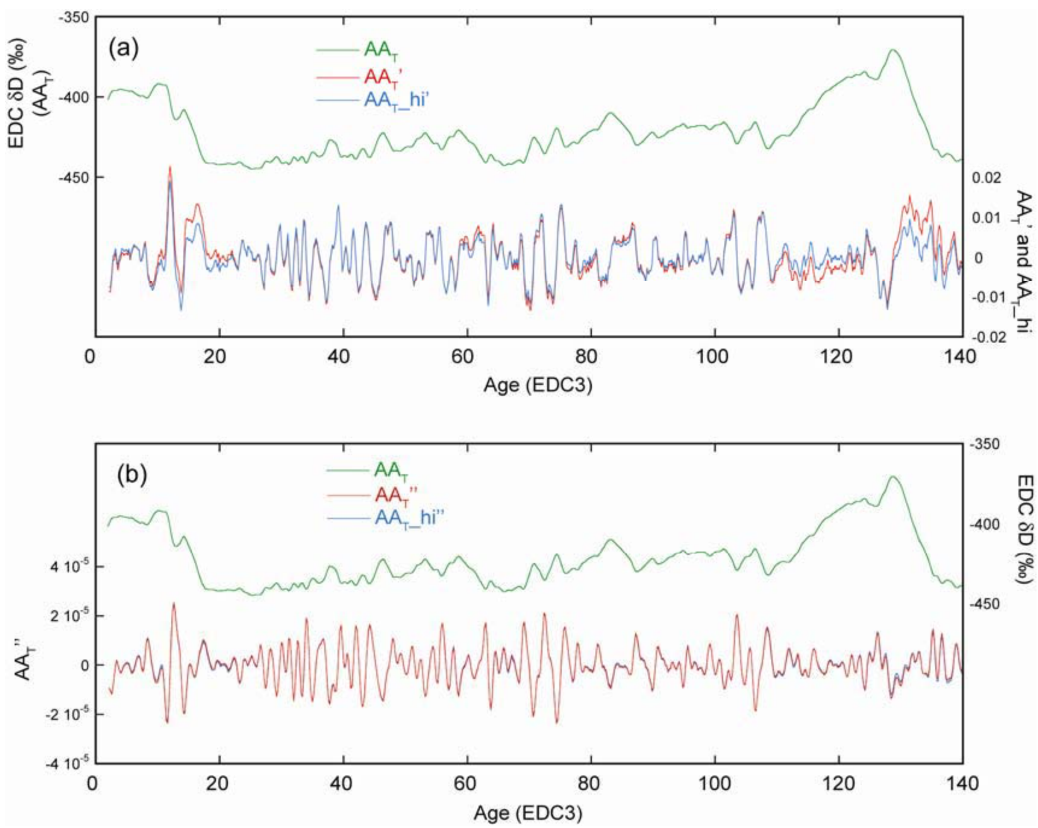

Figure S1. Effect of high-pass filtering on AA_T' and AA_T''. (a) The first differential (AA_T') is sensitive to the interplay between millennial- and orbital-timescale variations. The corresponding effect on the second differential (b) is minimal.

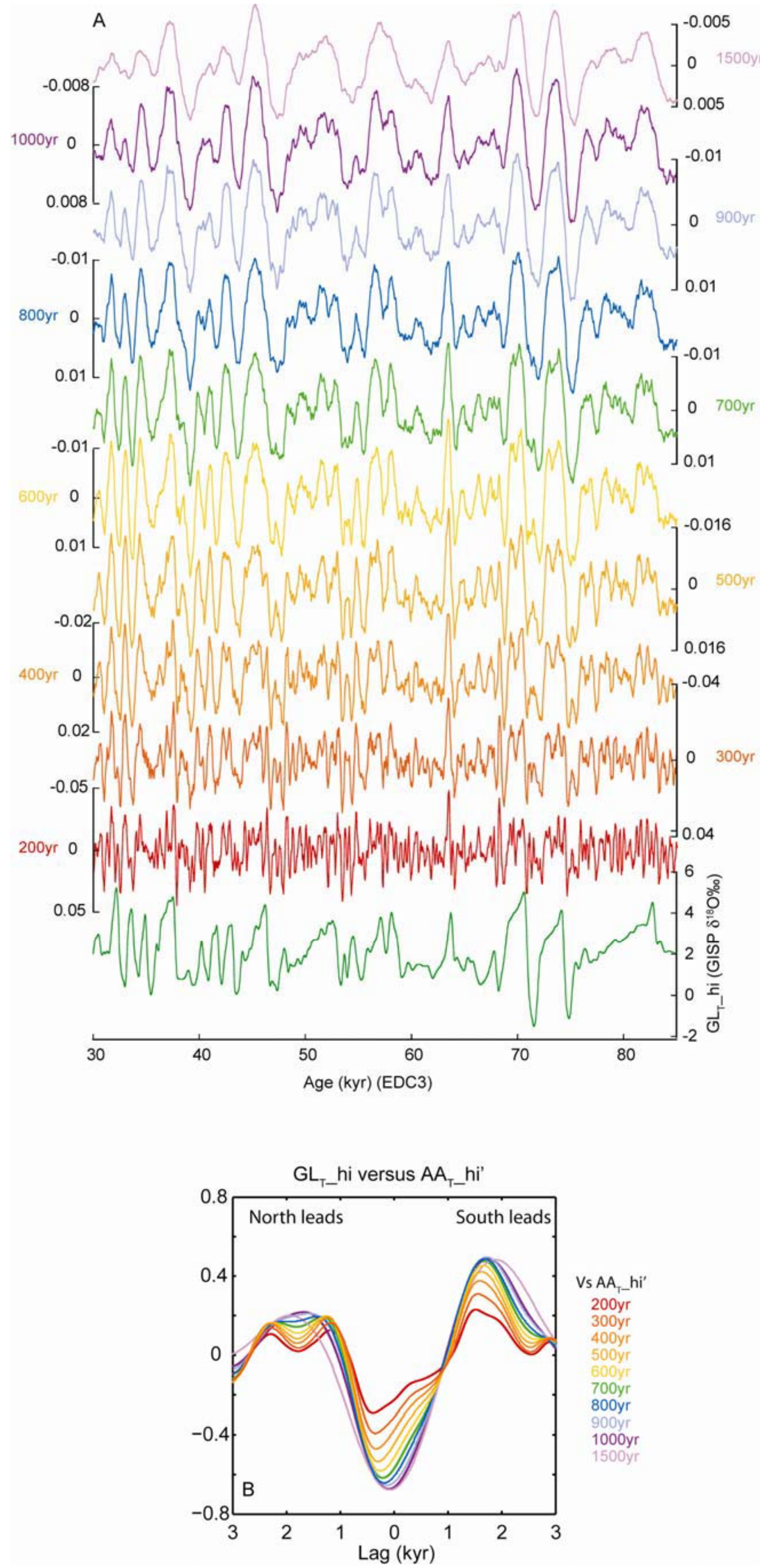

Figure S2. Smoothing of AA_T_hi before differentiating causes a reduction in noise but results in a reduction in the abruptness of predicted events as compared with the Greenland record. The choice of 700 years for the filter length is made based on compromise between optimal correlation between AA_T_hi' and GL_T_hi and the obliteration of certain features in the record (see also Fig. S3).

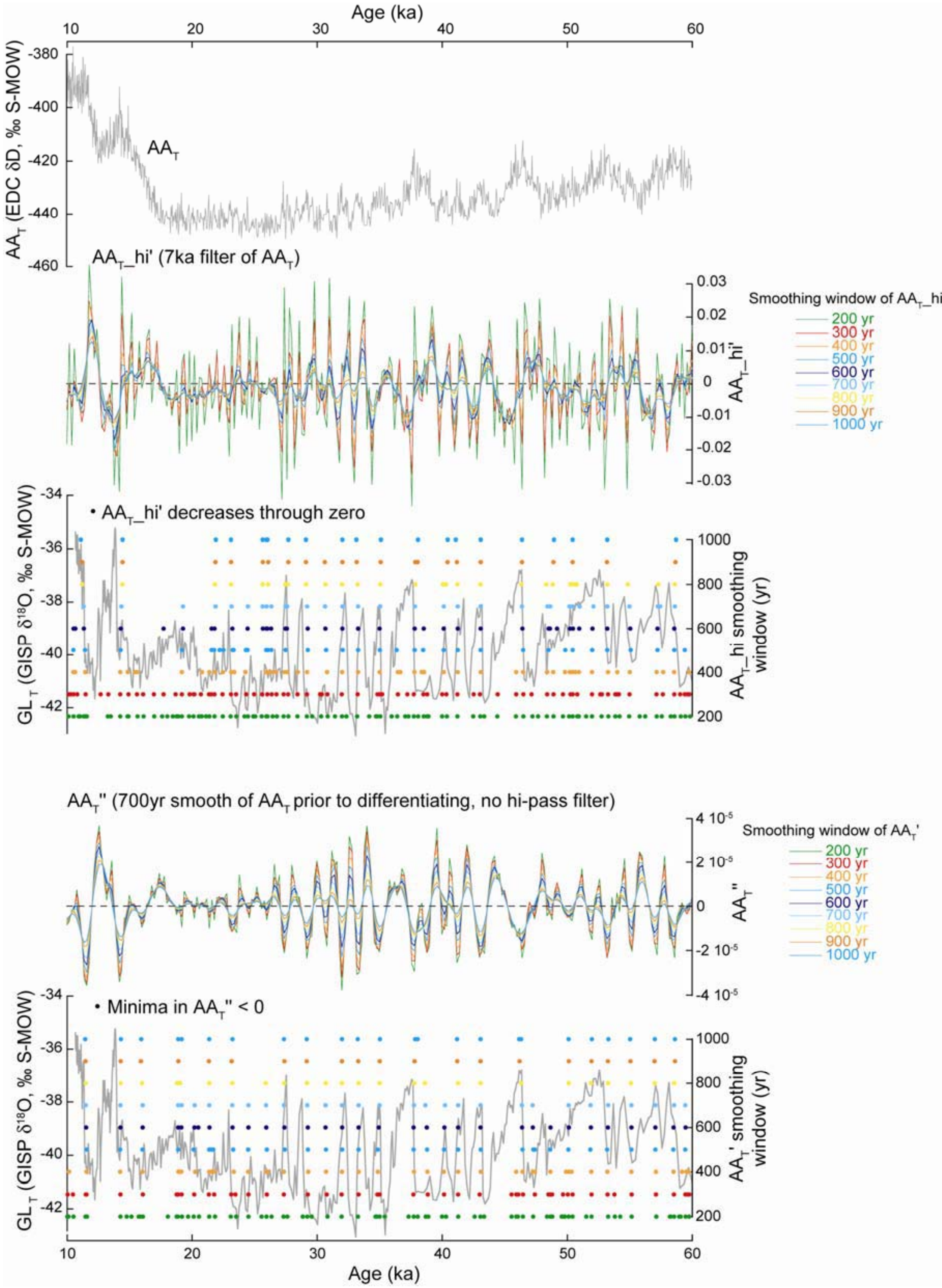

Figure S3. Abrupt warming events in Greenland are associated with AA_T_hi' decreasing through zero and minima in the record of AA_T''. Lower filter orders result in many events with no obvious correlatives in Greenland while higher order smoothing results in loss of events. The timing of significant events is not particularly sensitive to the choice of filter length.

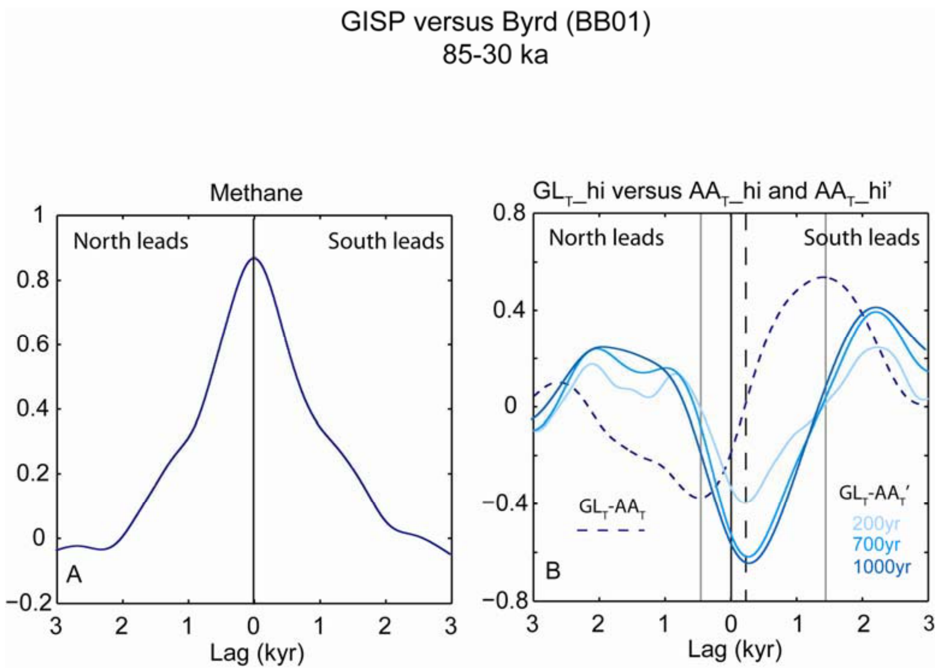

Figure S4. Cross correlations between records from the GISP 2 and Byrd ice cores as aligned by Blunier and Brook (*4*). (A) Methane correlation suggests that the tuning for gas phases is successful. (B) GL_T_hi versus AA_T_hi reveals the classic northern lead for an anti-correlation and southern lead for a positive correlation (*5, 33*). This may be contrasted with GL_T_hi versus AA_T_hi', which show an anti-correlation with approximately zero phase (the apparent ~200 year lead of AA_T_hi' over GL_T_hi is within the uncertainty in Δage). We find that an initial smooth of AA_T of 700 years (using a running mean, applied twice) gives optimal correlation with GL_T_hi whilst maintaining maximum detail in the derived record of AA_T_hi' (see also Fig. S2).

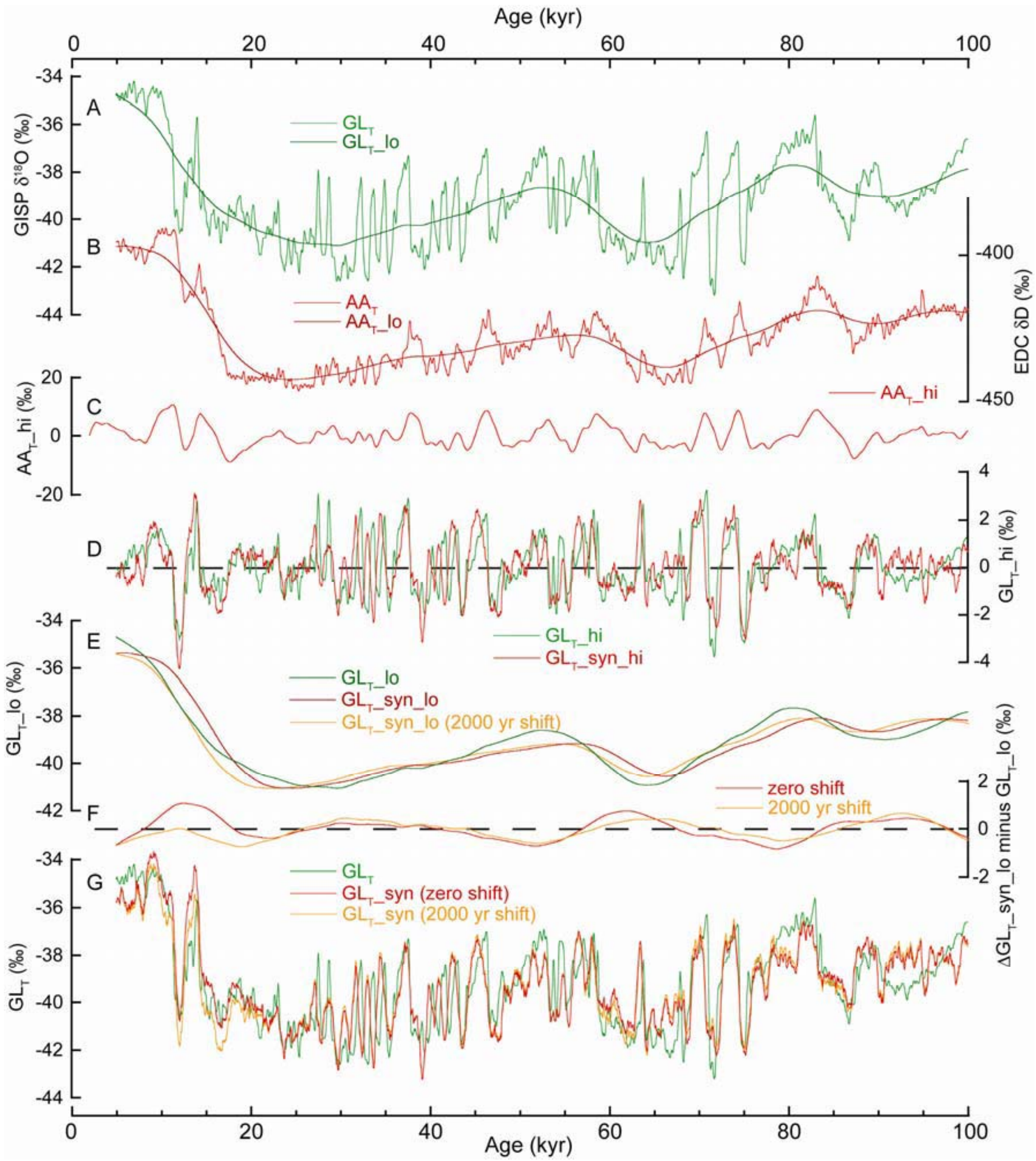

Figure S5. Construction of GL_T_syn. (A, B) the records of GL_T and AA_T respectively, with their orbital-timescale components, GL_T_lo and AA_T_lo. (C) the millennial-scale component of AA_T (AA_T_hi). (D) GL_T_syn_hi with GL_T_hi. (E) The orbital-timescale components, including a 2000 year shift of the Antarctic record. (F) Offsets between AA_T_lo and GL_T_lo with and without a 2000 year shift. (G) GL_T_syn (with and without a 2000 year shift) compared with GL_T.

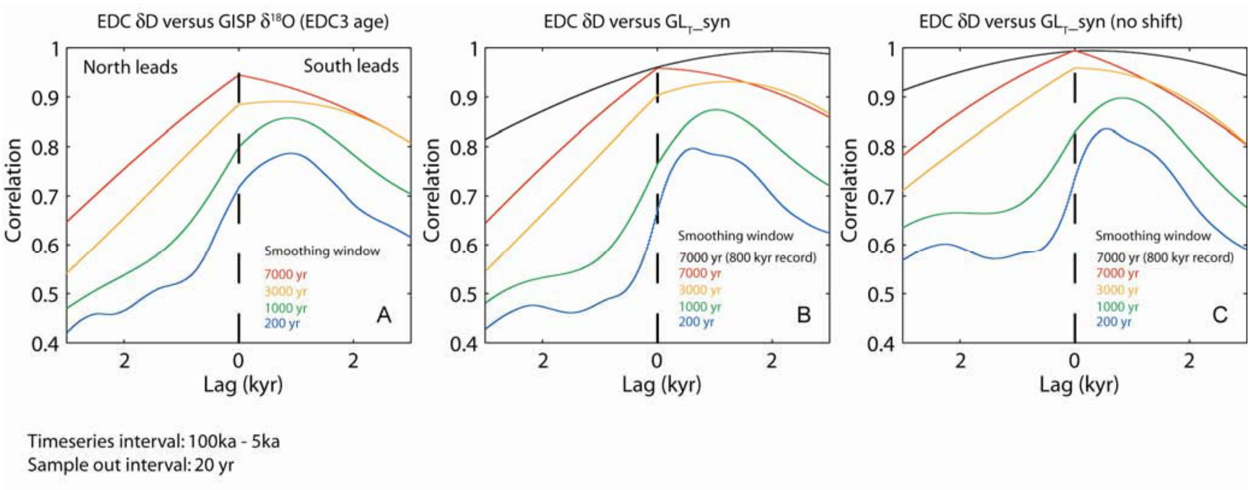

Figure S6. Lead lag correlations between GL_T and AA_T. (A) EDC δD versus GISP $\delta^{18}O$ for the interval 100 to 5 ka. A clear southern lead is observed for low order (200-1000 yr) smoothing of the records. The orbital-timescale components (7000 yr smooth; red curve) are highly correlated but the Greenland record is too short to allow a confident assessment of the relative phasing (maximum correlation is actually observed at zero lag but this is probably an artefact of the short record length relative to the smoothing window). (B) EDC δD versus GL_T_syn. In this case GL_T_syn is produced by adding GL_T_syn_hi to the scaled orbital-timescale component of AA_T (AA_T_lo) which has been shifted by 2000 years. The results for the interval 100 to 5 ka are very similar to panel (A) but now the records are long enough (~800 kyr; black curve) to allow observation of the 2000 year lag between the orbital components (a correlation of ~1 is obtained at a 2000 year lead of EDC δD over GL_T_syn). (C) EDC δD versus GL_T_syn where the orbital-timescale component of GL_T_syn has not been shifted. As expected, the correlation between the orbital-timescale components is a maximum at zero lag (black curve). Note also that for the interval 100 to 5 ka (red curve) the correlation is approximately symmetric about zero. This contrasts with the equivalent correlations in (A) and (B). We use this observation to support our inference that the orbital-timescale component of GISP $\delta^{18}O$ lags that of EDC δD by approximately 2000 years.

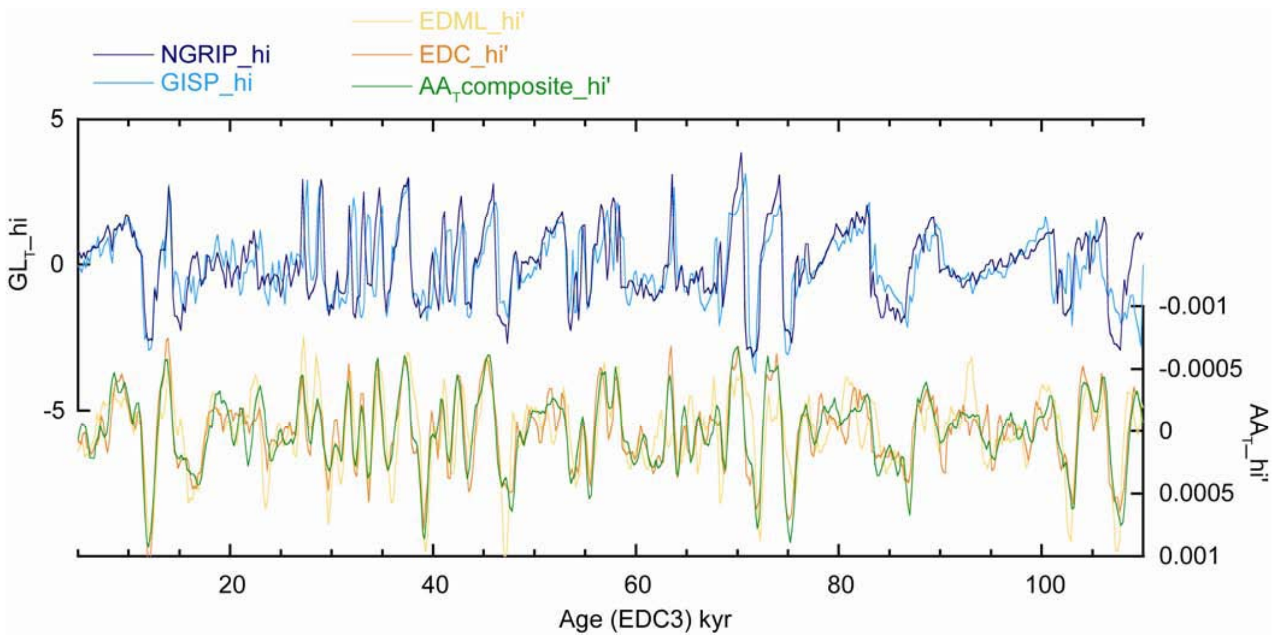

Figure S7. Comparison of the first differentials of EDC, EDML and a composite Antarctic record (derived by tuning and normalising the isotope records from EDC (*8*), EDML (*17*), Vostok (*11*), Dome Fuji (*18*) and Byrd (*19*)) with the millennial-scale components of the GISP (*20*) and NGRIP (*21*) ice cores. All records are on the EDC3 timescale. The GISP record was tuned via CH_4 (Fig.1) and the NGRIP $\delta^{18}O$ record was tuned directly to GL_T_syn.

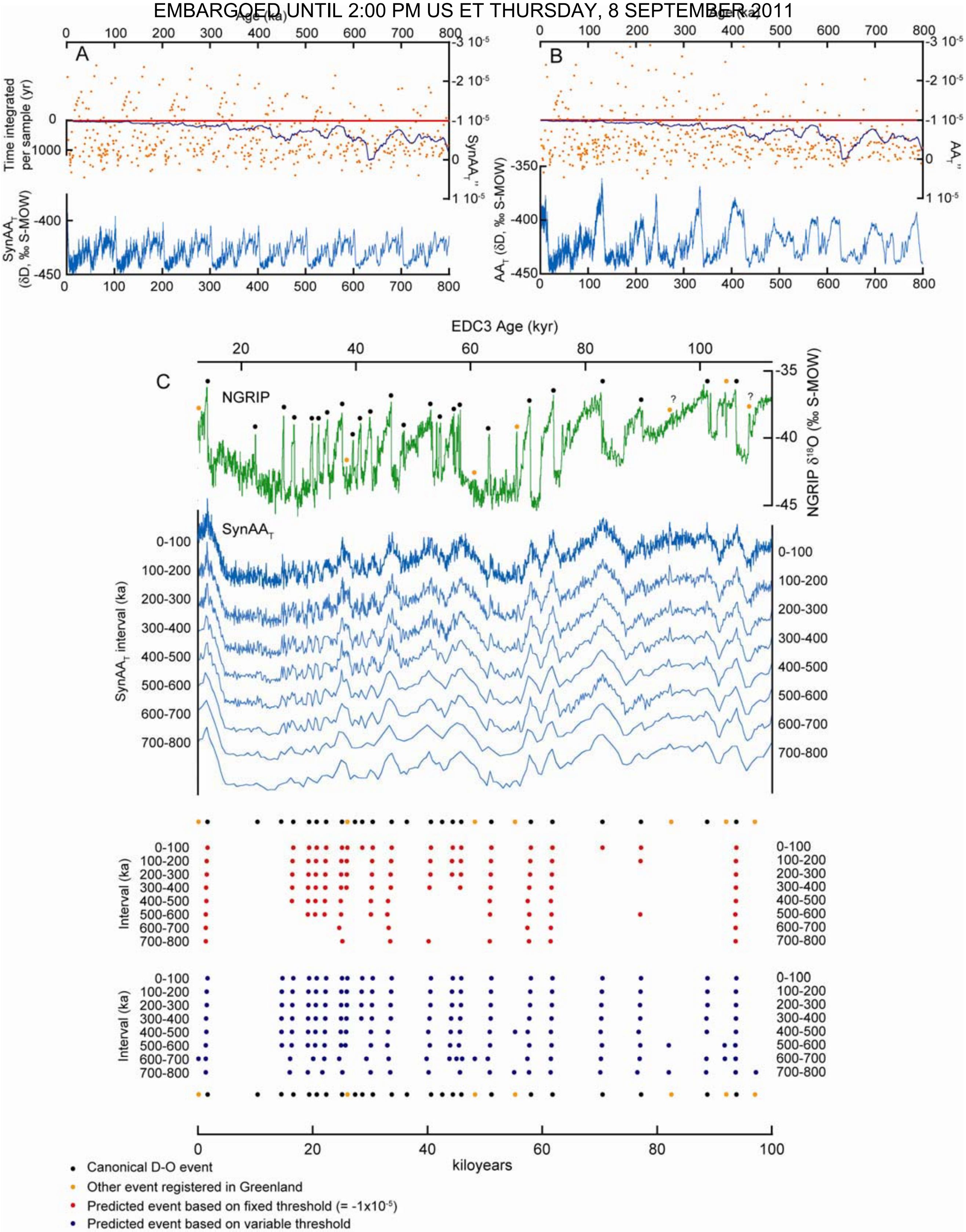

Figure S8. Accounting for signal attenuation using a synthetic ice core record. Panels (A) and (B) show the synthetic (A) and real (B) records of δD (light blue curves) for the last 800 kyr. For each record, the second differential (AA_T'') was calculated and the minima from each record are plotted as orange dots. With no loss of fidelity we would expect the minima in $SynAA_T$'' (the second differential of the synthetic record) to be repeated for each 100 kyr section of the record and this can clearly be seen for the upper 400 kyr. Thus we would expect to be able to pick the same D-O events for each repeated interval. However, increasing time-per-sample (integrated time per 55cm sample of ice) in deeper sections of the core (dark blue curves in A and B) causes a decrease in the amplitude of δD variability and a corresponding decrease in the amplitude of AA_T'' variability. This is revealed by a general reduction in the minimum values for deeper sections and means that many events would be missed if a fixed threshold (red line) was applied (red dots in panel C). We therefore allow the threshold to vary according to the time-per-sample (the variable threshold is the same dark blue curve as represents time-per-sample but its Y-axis is the same as that for AA_T''). (C) The synthetic ice core record is now used to assess the success of the variable threshold. The red dots in panel C are the picked D-O events using a fixed threshold. More and more events are lost with each progressive 100 kyr interval, reflecting the loss of fidelity in the record. The same should be expected if using the real δD record from EDC. By using a varying threshold most of the events identified for the upper sections can also be selected for deeper sections (blue dots in panel C). The same varying threshold is then used to predict the occurrence of D-O events for the real record of δD (main text Figs. 3, 4). The record of $\delta^{18}O$ from NGRIP (*21*) shown here has been tuned to our record of GL_T_syn (on the EDC3 timescale) in order to allow comparison between predicted versus canonical (plus other) events (recall that the synthetic record is a repeat of the EDC3 interval 12-112 ka).

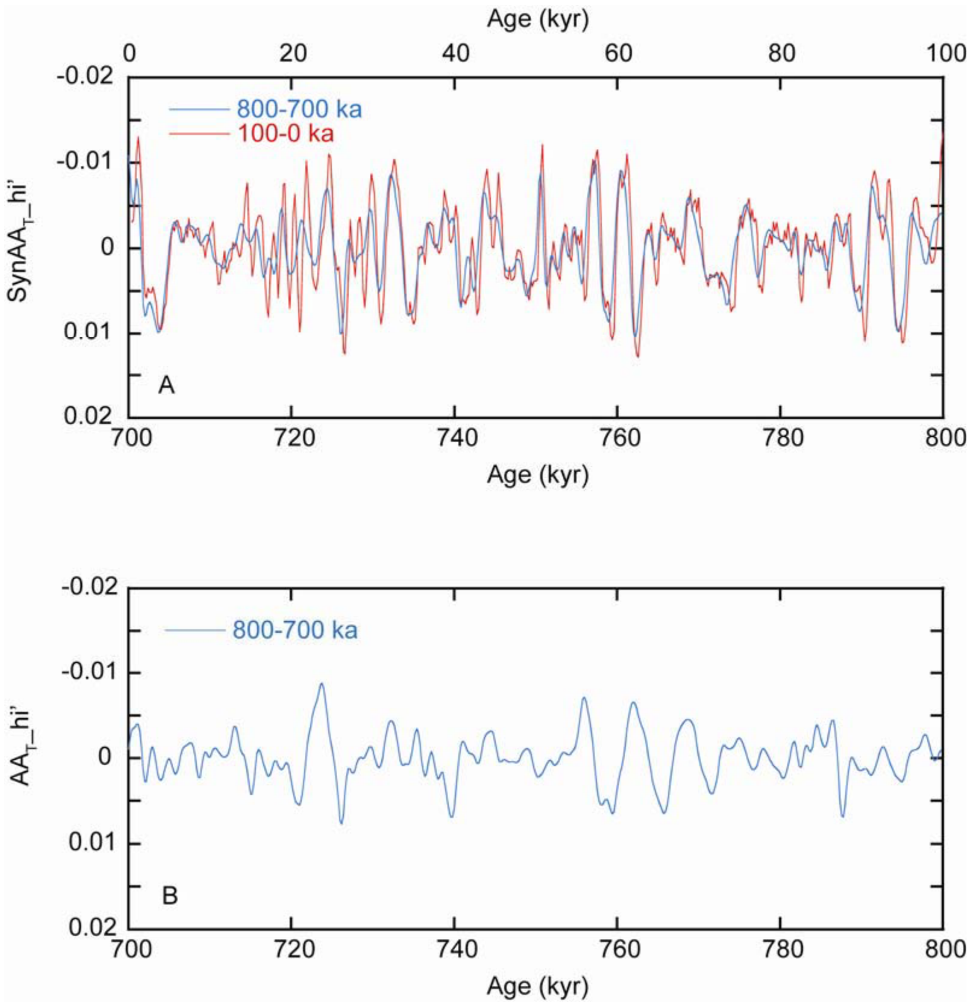

Figure S9. (A) Using the synthetic ice core record we can see that for shorter events (1-2 kyr) the increase in time-per-sample for deeper core sections results in a reduction in the amplitude of AA_T_hi' and total loss of some events. However, for long events (e.g. those during terminations) there is minimal reduction in the amplitude of AA_T_hi'. (B) Based on this we argue that there should be minimal loss of amplitude in AA_T_hi' for longer events in the deeper sections of the actual EDC δD record.

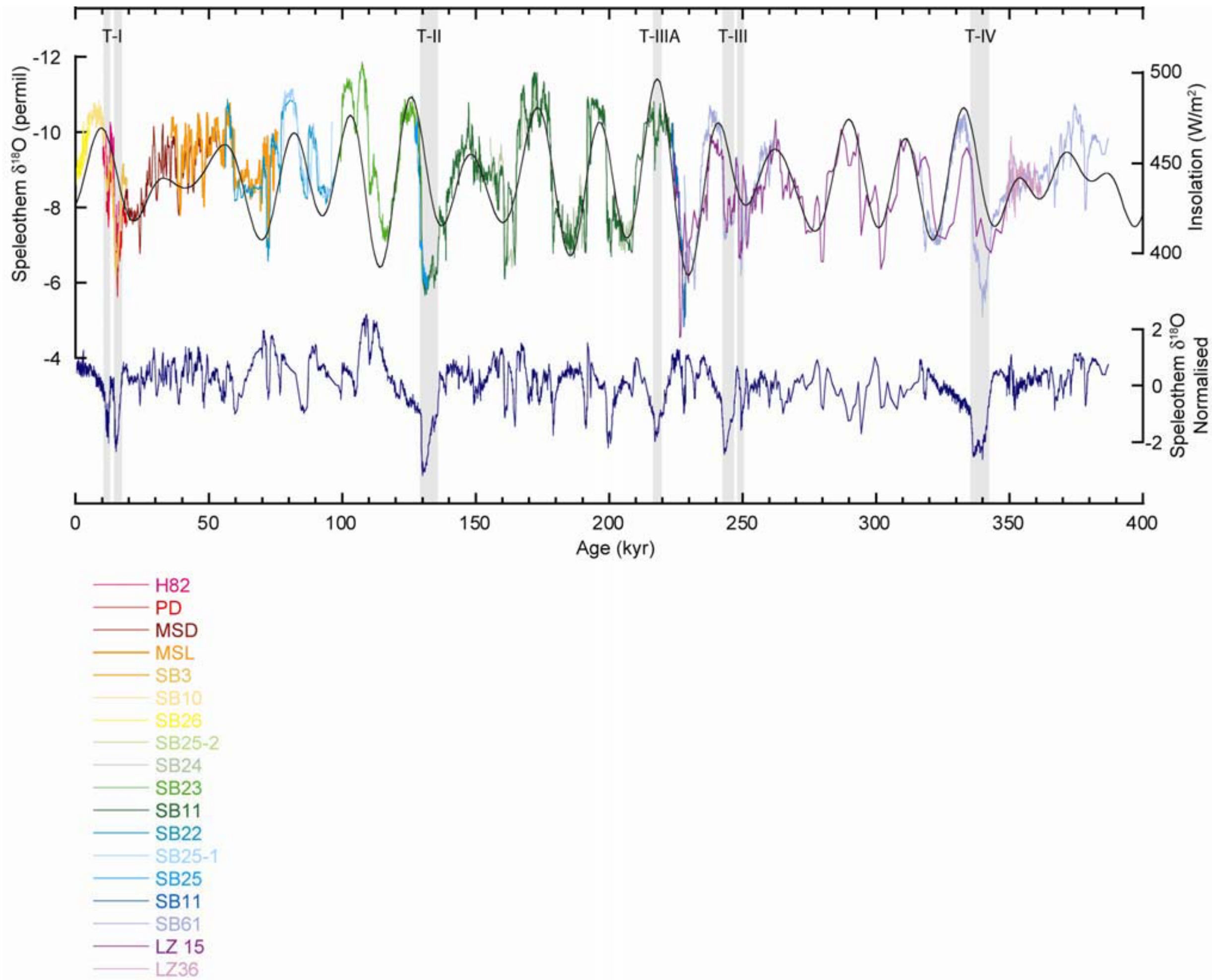

Figure S10. Normalisation of the Chinese speleothem record (*24, 31, 32*) to the record of insolation for July 21 at 65ºN (*34*) highlights the nature of millennial-scale variability within this record.

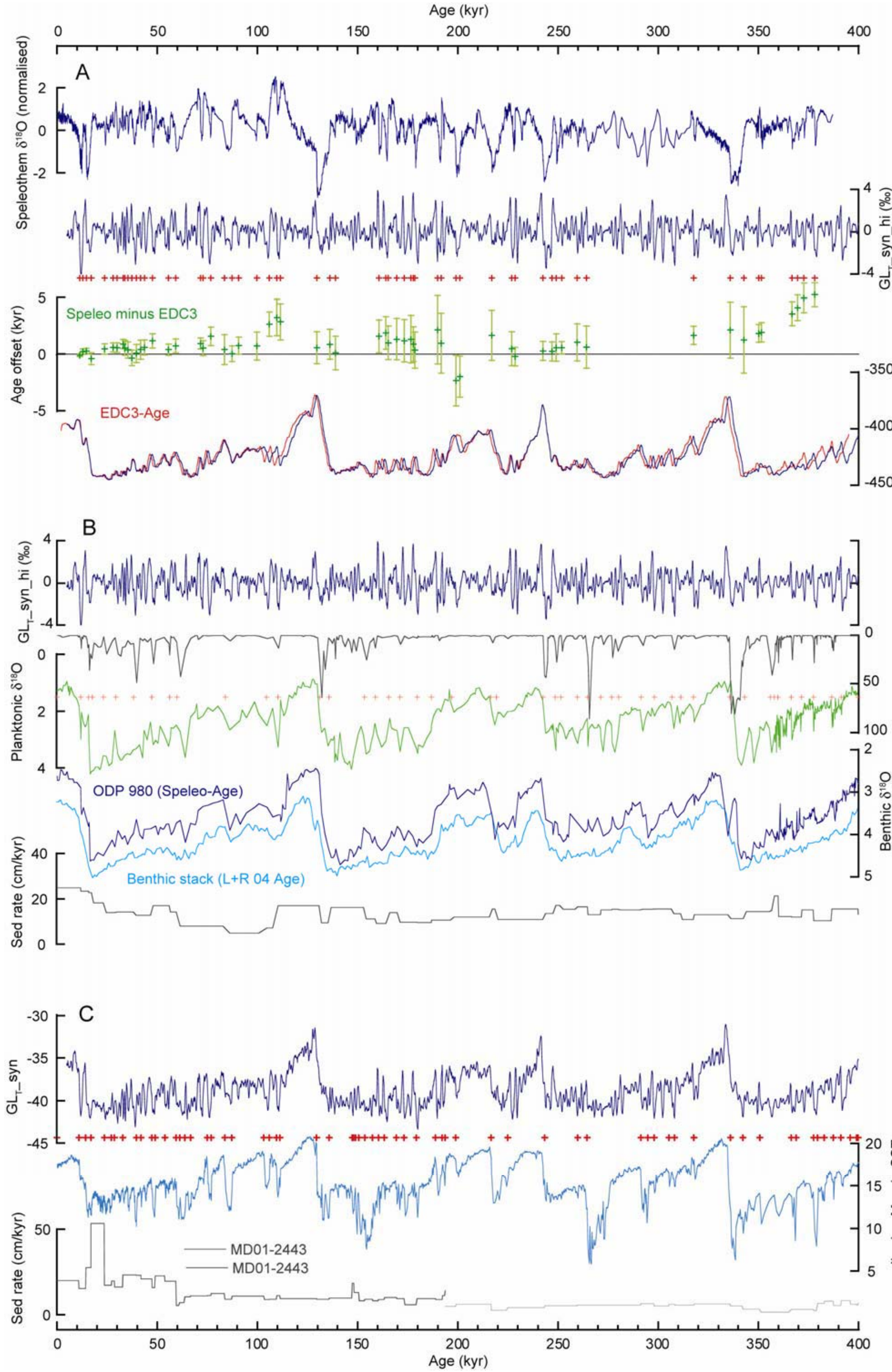

Age (kyr)
A
Speleothem δ18O (normalised)
GLT_syn_hi (‰)
Speleo minus EDC3
Age offset (kyr)
EDC3-Age
B
GLT_syn_hi (‰)
Planktonic δ18O
IRD(%) (980)
ODP 980 (Speleo-Age)
Benthic δ18O
Benthic stack (L+R 04 Age)
Sed rate (cm/kyr)
C
GLT_syn
Iberian Margin SST
Sed rate (cm/kyr)
MD01-2443
MD01-2443
Age (kyr)

Figure S11 (previous page). (A) Tuning GL_T_syn_hi to the detrended speleothem record. Tuning points are indicated by red crosses. The deviation of our age model ('Speleo-Age') from the published EDC3 age model (*27*) is generally less than ~2kyr. Error bars are total estimated uncertainty in our absolute age points. (B) Tuning ODP 980 to GL_T_syn_hi (and GL_T_syn) via the records of planktonic foraminiferal $\delta^{18}O$ and %IRD(*28*) (red crosses are tuning points). The corresponding record of benthic $\delta^{18}O$ from the same core (on our new timescale) shows good correspondence with the benthic $\delta^{18}O$ stack published by (*35*). Also shown is the implied sedimentation rates for ODP 980. (C) The alkenone record of Iberian Margin SST (*29*) tuned to our record of GL_T_syn.

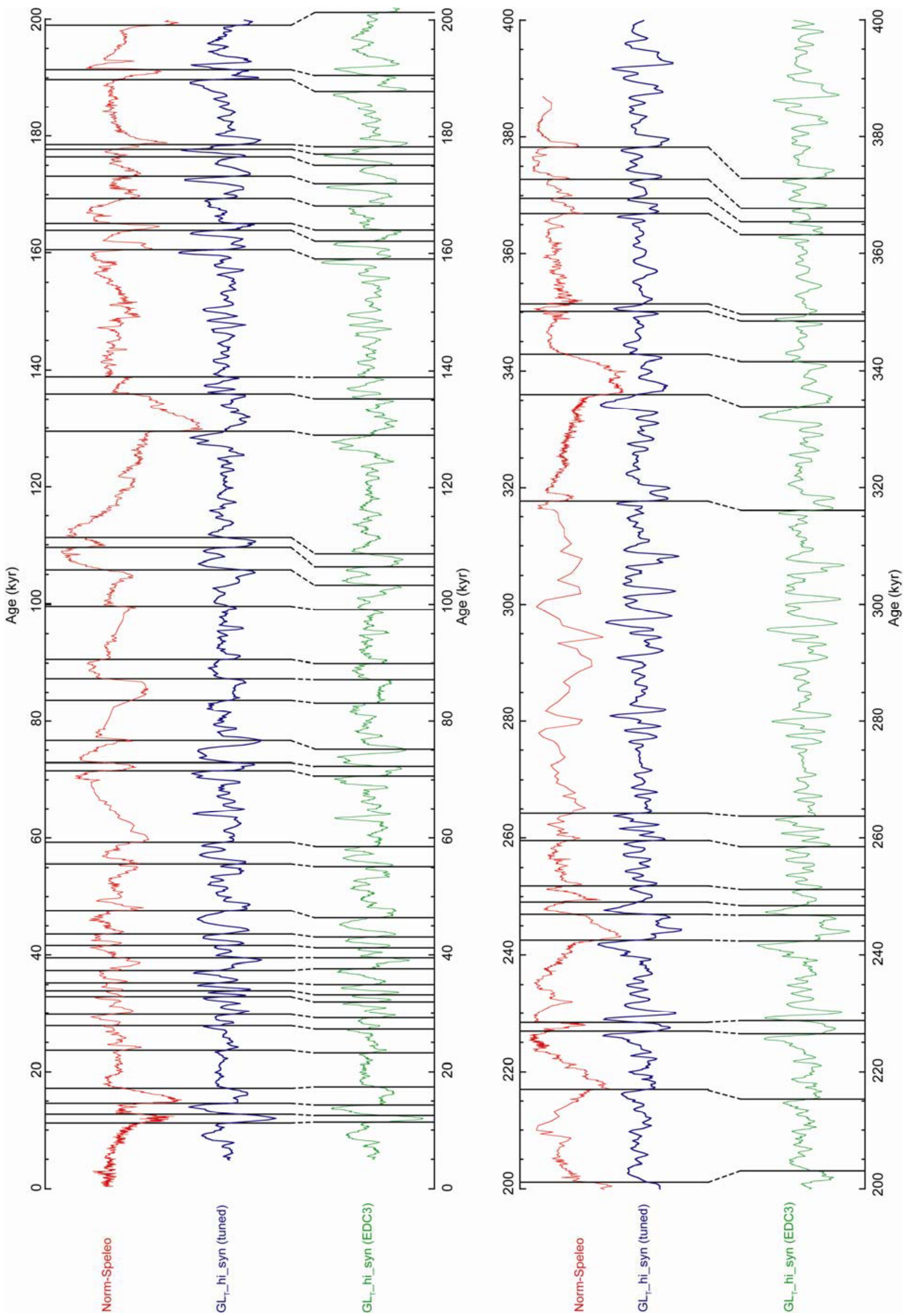

Figure S12. Detail of tuning between GL_T_syn_hi and the normalised speleothem record. No attempt is made to tune within the interval ~315 to 265 kyr, due to the lower resolution of the speleothem record at this time. Tuning points are given in Table S1.

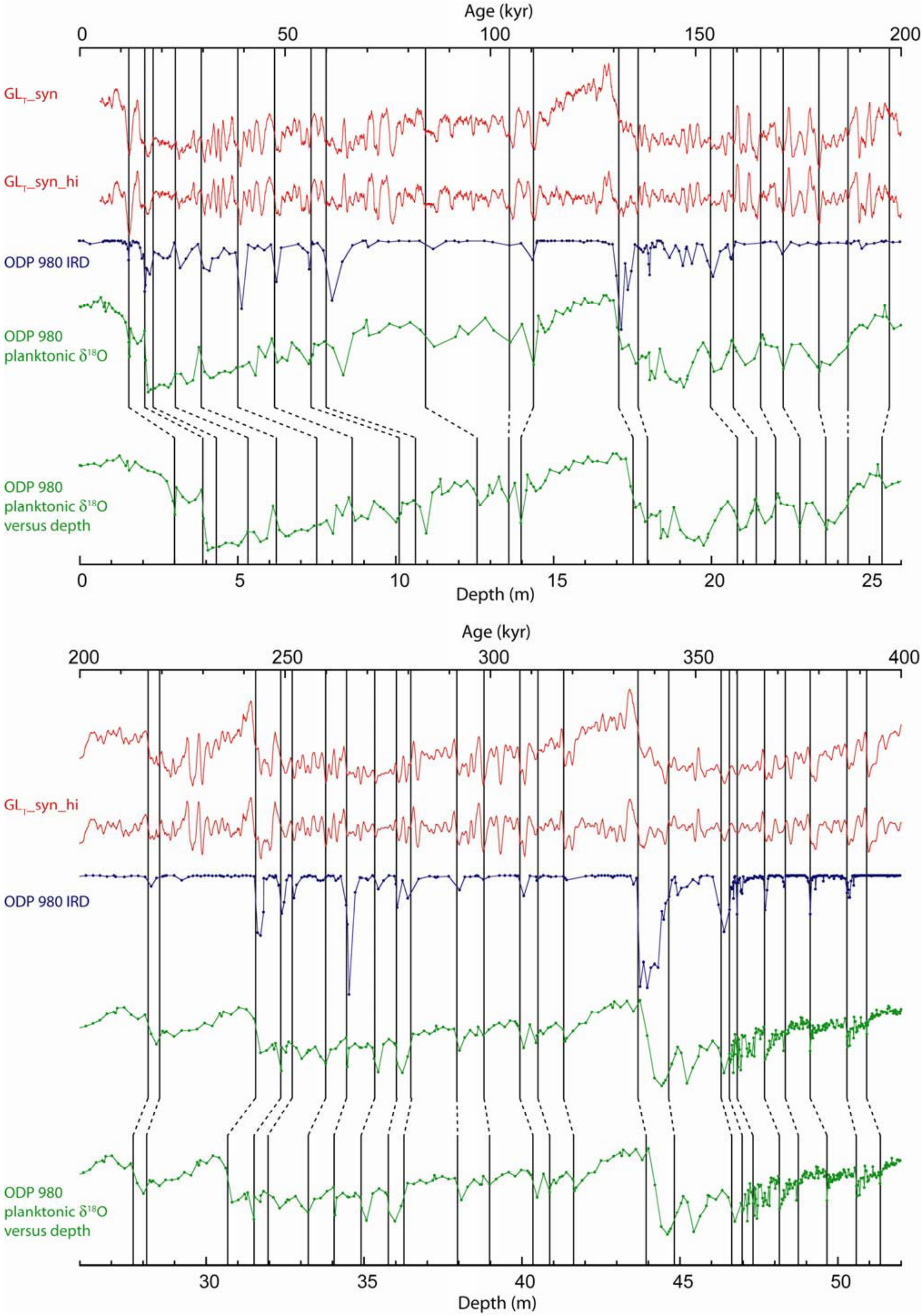

Figure S13. Detail of the tuning between ODP 980 (*28*) and GL$_T$_syn. Note that the records of both %IRD and planktonic foraminiferal δ^{18}O from ODP 980 were used for this exercise.

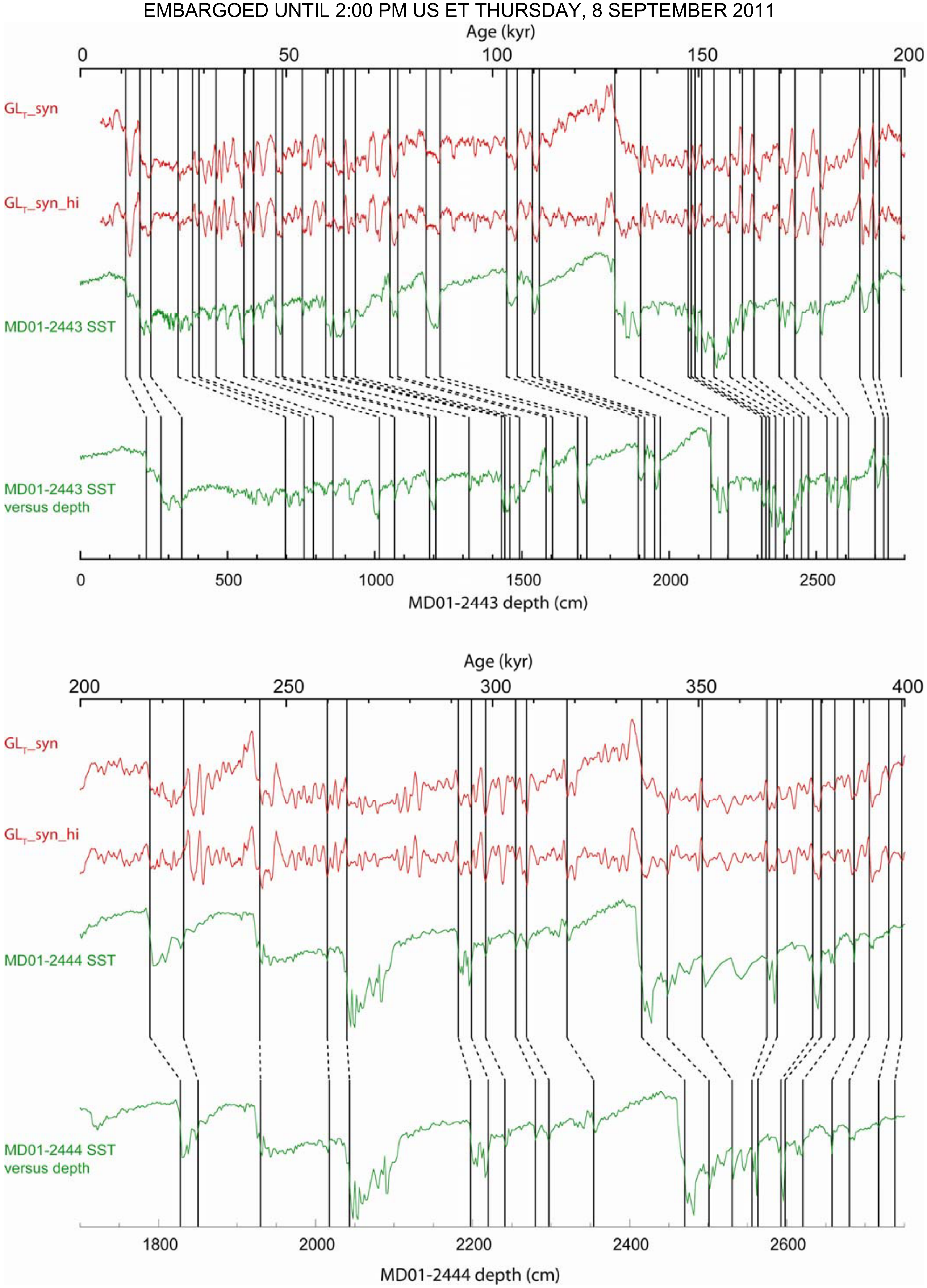

Figure S14. Detail of the tuning between the Iberian Margin SST record (*29*) and GL$_T$_syn

EDC3 age (kyr)	SpeleoAge (kyr)	Dage (kyr)	Tuning error (kyr)	Absolute speleo error (kyr)	Combined uncertanty (kyr)
11.47	11.36	-0.11	0.11	0.08	0.14
12.58	12.80	0.22	0.22	0.10	0.24
14.34	14.62	0.27	0.21	0.10	0.23
17.52	17.11	-0.40	0.50	0.10	0.51
23.29	23.77	0.47	0.42	0.15	0.45
27.40	28.00	0.60	0.36	0.19	0.41
29.33	29.90	0.57	0.36	0.21	0.42
32.04	32.94	0.90	0.25	0.33	0.41
33.35	33.90	0.55	0.36	0.54	0.65
35.00	35.38	0.38	0.34	0.63	0.71
37.76	37.43	-0.33	0.25	0.63	0.68
39.50	39.58	0.07	0.34	0.73	0.80
41.30	41.70	0.40	0.42	0.73	0.84
43.13	43.72	0.60	0.36	0.55	0.66
46.42	47.60	1.17	0.22	0.59	0.63
55.20	55.60	0.40	0.22	0.45	0.50
58.58	59.30	0.72	0.36	0.50	0.62
70.70	71.63	0.94	0.28	0.40	0.49
72.40	72.93	0.53	0.42	0.50	0.66
75.18	76.75	1.57	0.50	0.65	0.82
83.20	83.60	0.40	1.08	0.75	1.31
87.32	87.35	0.04	0.34	0.60	0.69
89.93	90.67	0.75	0.36	0.65	0.74
99.06	99.77	0.71	0.58	1.10	1.24
103.31	105.97	2.65	0.50	0.95	1.07
106.52	109.76	3.24	0.35	1.55	1.59
108.69	111.54	2.85	0.54	1.50	1.59
129.00	129.57	0.57	0.67	1.25	1.42
135.22	136.09	0.87	0.42	1.25	1.32
138.93	139.03	0.10	0.32	1.45	1.48
159.09	160.67	1.57	0.42	1.40	1.46
162.18	164.05	1.88	0.50	1.35	1.44
164.22	165.22	1.00	0.47	1.40	1.48
168.21	169.53	1.33	0.28	1.80	1.82
172.07	173.25	1.18	0.50	1.80	1.87
175.20	176.53	1.33	0.86	1.90	2.09
177.00	177.88	0.88	0.28	1.50	1.53
178.30	178.65	0.35	0.57	1.50	1.60
187.84	189.98	2.14	1.52	2.60	3.01
190.72	191.69	0.97	0.50	2.60	2.65
201.40	199.06	-2.35	0.42	2.20	2.24
203.12	201.13	-1.99	0.61	1.70	1.81
215.32	216.97	1.66	0.54	2.15	2.22
226.41	226.90	0.49	1.39	0.55	1.50
228.75	228.54	-0.22	0.42	0.70	0.82
242.27	242.55	0.28	0.81	0.25	0.85
246.75	246.99	0.24	0.78	0.30	0.84
248.46	249.04	0.57	1.17	0.30	1.21
251.28	251.85	0.58	0.50	0.20	0.54
258.52	259.56	1.04	0.57	1.55	1.65
263.62	264.24	0.62	1.04	1.55	1.87
316.04	317.70	1.66	0.40	0.70	0.81
333.83	335.96	2.13	1.30	2.10	2.47
341.56	342.83	1.27	2.04	2.10	2.93
348.43	350.26	1.83	0.28	0.75	0.80
349.59	351.53	1.94	0.28	0.80	0.85
363.26	366.82	3.57	0.36	1.00	1.06
365.40	369.50	4.10	0.50	1.00	1.12
367.79	372.75	4.96	0.50	1.20	1.30
372.90	378.15	5.25	0.30	1.00	1.04

Table S1 Age control points for placing the EDC records on the absolute age scale of speleothem records. Tuning errors are estimated from the widths of the selected transitions. Absolute speleothem errors are calculated from the quoted errors given for the nearest dated samples bracketing the selected tie point in the speleothem record (*24, 31, 32*).